Top Curr Chem (2014) 350: 1–64
DOI: 10.1007/128_2012_414

Published online: 29 March 2013

Buckyballs

Juan L. Delgado, Salvatore Filippone, Francesco Giacalone, Mª Ángeles Herranz, Beatriz Illescas, Emilio M. Pérez, and Nazario Martín

Abstract Buckyballs represent a new and fascinating molecular allotropic form of carbon that has received a lot of attention by the chemical community during the last two decades. The unabating interest on this singular family of highly strained carbon spheres has allowed the establishing of the fundamental chemical reactivity of these carbon cages and, therefore, a huge variety of fullerene derivatives involving [60] and [70]fullerenes, higher fullerenes, and endohedral fullerenes have been prepared. Much less is known, however, of the chemistry of the uncommon non-IPR fullerenes which currently represent a scientific curiosity and which could pave the way to a range of new fullerenes. In this review on buckyballs we have mainly focused on the most recent and novel covalent chemistry of fullerenes involving metal catalysis and asymmetric synthesis, as well as on some of the most significant advances in supramolecular chemistry, namely H-bonded fullerene assemblies and the search for efficient concave receptors for the convex surface of fullerenes. Furthermore, we have also described the recent advances in the macromolecular chemistry of fullerenes, that is, those polymer molecules endowed

J.L. Delgado and E.M. Pérez
IMDEA-Nanoscience, Campus de Cantoblanco, 28049 Madrid, Spain

S. Filippone, Mª.Á. Herranz and B. Illescas
Facultad de Química, Departamento de Química Orgánica, Universidad Complutense, 28040 Madrid, Spain

F. Giacalone
Universitá degli Studi di Palermo, Dipartimento di Scienzie e Tecnologie Biologiche, Chimiche e Farmaceutiche, Palermo, Italy

N. Martín (✉)
Facultad de Química, Departamento de Química Orgánica, Universidad Complutense, 28040 Madrid, Spain

IMDEA-Nanoscience, Campus de Cantoblanco, 28049 Madrid, Spain
e-mail: nazmar@quim.ucm.es

with fullerenes which have been classified according to their chemical structures. This review is completed with the study of endohedral fullerenes, a new family of fullerenes in which the carbon cage of the fullerene contains a metal, molecule, or metal complex in the inner cavity. The presence of these species affords new fullerenes with completely different properties and chemical reactivity, thus opening a new avenue in which a more precise control of the photophysical and redox properties of fullerenes is possible. The use of fullerenes for organic electronics, namely in photovoltaic applications and molecular wires, complements the study and highlights the interest in these carbon allotropes for realistic practical applications. We have pointed out the so-called non-IPR fullerenes – those that do not follow the isolated pentagon rule – as the most intriguing class of fullerenes which, up to now, have only shown the tip of the huge iceberg behind the examples reported in the literature. The number of possible non-IPR carbon cages is almost infinite and the near future will show us whether they will become a reality.

Keywords Asymmetric synthesis · Endohedral fullerenes · Fullerenes · Macromolecular chemistry · Molecular wires · Non-IPR fullerenes · Organic photovoltaics · Supramolecular chemistry

Contents

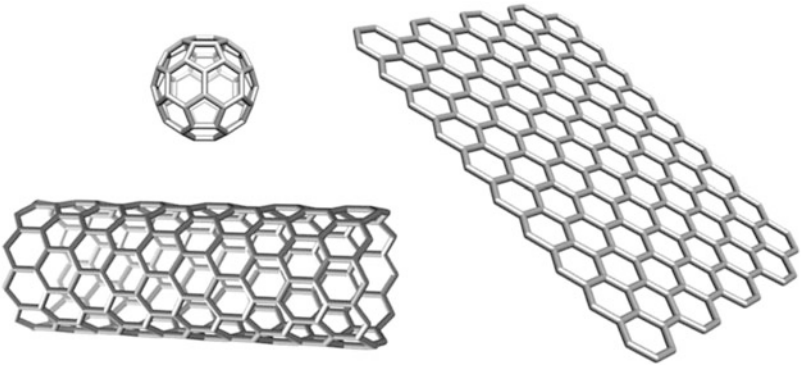

Fig. 1 Chemical structure of C_{60}, a single wall carbon nanotube and graphene

1 Introduction

From the 118 elements which have been identified according to the periodic table, only 94 elements are naturally occurring on earth while the remainder are considered artificial elements. Among the natural elements, carbon is the only one providing the basic requirements for life. Its ability of hybridization of atomic orbitals to produce sp^3, sp^2, and sp hybrid orbitals confers upon it the singular property of having a variety of allotropic forms. Surprisingly, it is less than three decades since only two allotropes of carbon, namely diamond – constituted by sp^3 carbon atoms – and graphite – formed by sp^2 carbon atoms – were known by the scientific community. Both allotropes show a reticular structure with carbon atoms spreading infinitely through the three space directions.

A new scenario emerged in 1985 with the advent of fullerenes, the third and only molecular allotropic form of carbon, formed by highly symmetric closed cages of a well-defined number of carbon atoms [1]. Interestingly, fullerenes have been present on our planet from its very beginning as well as in outer space (the presence of fullerenes C_{60} and C_{70} has recently been detected by IR in huge amounts in a young planetary nebula (Tc 1). The fullerene content is around 1.5% of the carbon present in the nebula, roughly corresponding to the mass of three moons [2]).

Soon after the discovery of fullerenes, other important different forms of carbon were found, namely, in chronological order, multiwall [3] and singlewall [4, 5] carbon nanotubes, and most recently graphenes [6] which have provoked great excitement and expectation in the scientific community (Fig. 1). In the meantime, a wide variety of other less common nanoforms of carbon also emerged such as nanohorns, nanoonions, nanotori, nanobuds, peapods, etc., whose properties and chemical reactivity are less well known to date [7]. Furthermore, fullerenes have been skillfully combined with other elements allocated to their inner empty space, affording a large, singular, and promising family of *so-called* endohedral fullerenes – those containing an atom, molecule, or complex in their inner cavity – whose properties and chemical reactivity are strongly influenced by the elements inside the ball [8].

The increasing number of nanoforms of carbon gives rise to a first taxonomic problem. Should the aforementioned nanoforms of carbon be considered as different allotropes? Answering this question could be accomplished by considering the IUPAC definition of allotrope as "the different structural modifications of an element" (IUPAC Compendium of Chemical Terminology, 2nd edition, 1997). Although at a first glance they could be considered as different allotropes, the scientific community considers fullerenes as the third allotropic form of carbon in which the sp^2 carbon atoms are bonded to form spherical, tubular, or ellipsoid structures, thus gathering all the above forms within the same allotrope of "fullerenes."

The above considerations do not, however, affect "buckyballs," a nickname which refers only to the former fullerenes, that is, those constituted exclusively by closed cages of a precise number of carbon atoms, the most representative examples being C_{60} and C_{70} molecules, and the most abundant and easy to obtain fullerenes. In this chapter we will discuss the properties, chemical reactivity, and some of the most realistic applications of fullerenes, including endohedral fullerenes and those rare fullerenes which do not follow the "isolated pentagon rule" (see below).

1.1 Brief History of Fullerenes

The discovery of fullerenes represents one of the most recent examples of serendipity in chemistry. Fullerenes were discovered by Robert F. Curl, Sir Harold W. Kroto, and the late Richard E. Smalley in 1985 [1] during carbon nucleation studies under red giant star conditions. Only 11 years later, in 1996, these scientists were awarded the Nobel Prize in Chemistry for "the discovery of fullerenes" [9–11]. Just a year before, C_{60} had been declared the molecule of the year by the scientific journal *Science*.

This important finding has resulted in a new field with a broad impact in science, thus provoking great excitement in the scientific community, ranging from chemistry, physics, and engineering to practical applications in materials science and biomedical applications [12]. Actually, the impact of the new fullerenes goes beyond the scientific world and, since this molecule was first found in Texas, the State Parliament declared Buckminsterfullerene C_{60} the molecule of Texas State in May 1997.

However, a major breakthrough in fullerene science occurred in 1990 when Wolfgang Krätschmer and Donald Huffman (two astrophysicists) prepared fullerene C_{60} for the first time in multigram amounts [13] thus opening the fullerene world to chemical functionalization and, therefore, to the unlimited imagination of chemists for synthesizing new and sophisticated fullerene architectures. The importance of this achievement was pointed out by some of the Nobel laureate scientists. In Smalley's own words: "Had there not been a method to make it in measurable amounts, it would not have had an impact." Curl also recognized this scientific

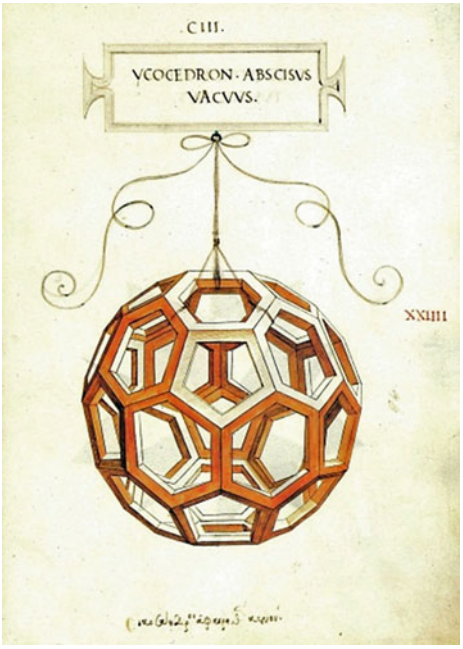

Fig. 2 Ycocedron Abscisus Vacuus by Leonardo da Vinci

contribution, stating: "Huffman's work took it from mass spectrometers to the laboratory. It must have been a close decision by the Nobel committee over who should get it."

However, the history of fullerenes started many years before. Actually, the possible existence of the C_{60} molecule was proposed 15 years before its discovery by Eiji Osawa from Kyoto University. Kroto who did not know this work at the time of discovery, in part due to its publication in Japanese, has given great credit to this Japanese scientist.

The idea of a closed carbon cage was initially proposed by David E.H. Jones in 1966 in an article written in the *New Scientist* under the name "Daedalus" [14]. He suggested that giant empty cages could be formed by distorting a planar net of hexagonal carbons (a vision of graphene?) by adding impurities. However he was never able to explain how it could be done. It is interesting to note, nevertheless, that in situ TEM experiments correlated with quantum chemical modeling have demonstrated that flat graphene sheets undergo a direct transformation to fullerene cages under 80-keV electron beam irradiation [15].

Some more romantic chemists have seen in Leonardo da Vinci's work the first scientific "modeling" of the C_{60} molecule in his famous illustration for the book by Luca Pacioli entitled "De Divina Proportione," published in Venice in 1509. In this illustration the truncated icosahedron called "Ycocedron Abscisus Vacuus" by Leonardo is shown (Fig. 2).

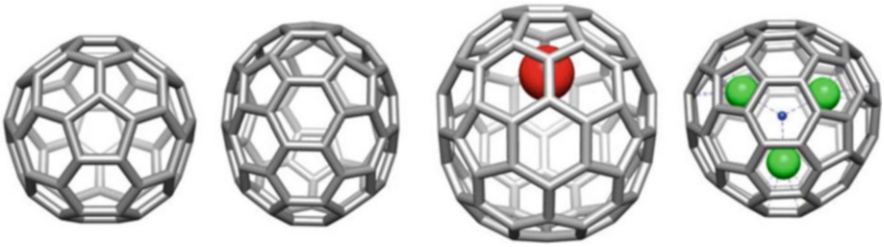

Fig. 3 Empty fullerenes C_{60} and C_{70} (*left*) and endohedral fullerenes La@C_{82} and Sc_3N@C_{80} (*right*)

1.2 General Remarks on the Chemical Reactivity of Fullerenes

Buckyballs constitute a family of closed cage carbon allotropes that contains 2 (10 + *H*) carbon atoms, where *H* is the number of hexagons, while the number of pentagons is always fixed at 12. In principle, an unlimited number of fullerene structures could result. However, the simplest and most abundant is C_{60}, which is formed by 60 carbon atoms –12 pentagons and 20 hexagons–, followed by C_{70}. C_{60} has icosahedral symmetry and a diameter of 7.8 Å. An important structural motif of fullerenes is the so-called "isolated pentagon rule," which means that all pentagons in the molecule must be isolated from other pentagons, since structures with fused pentagons are highly destabilized due to the increase in strain energy and resonance destabilization [16] (Fig. 3).

In contrast to diamond and graphite, which are sparingly soluble in organic solvents, fullerenes are soluble in some organic solvents. They undergo a variety of chemical reactions in solution to afford a huge number of fullerene derivatives which, in general, preserve the outstanding chemical, physical, and electrochemical properties of pristine fullerenes. The study of the chemical reactivity of fullerenes has experienced an unprecedented development during the last two decades and is expected to continue on this steep slope.

The singular 3D geometry of fullerenes containing 30 or more highly reactive double bonds constitutes a new scenario where a variety of different chemical reactions can be tested. The convex surface of fullerenes offers new possibilities for the study of new reactions and mechanisms under severe geometrical constraints on carbon atoms showing a singular $sp^{2.3}$ hybridization [17].

The contributions stemming from well-established and versatile protocols to functionalize fullerenes chemically have yielded a broad spectrum of intriguing, tailor-made fullerene derivatives. The remarkable properties of the latter are continuously under investigation and form the basis in the search for practical applications of fullerenes.

As mentioned above, the C_{60} molecule is formed from 12 pentagons and 20 hexagons linked by single and double carbon–carbon bonds. The calculated bond distances reveal subtle differences between the [5,6]- and [6,6]-bonds with values of 1.45 and 1.38 Å, respectively. Due to the mixed character of 1,3,5-cyclohexatrienes

and [5]radialenes, C_{60} behaves as a highly strained electron-poor alkene. The chemical reactivity is mainly driven by strain relief and, therefore, addition reactions have been widely used [18]. Interestingly, although similar reactivity patterns have also been observed for higher fullerenes, chemical reactivity tends to decrease significantly with their size [19–21].

A variety of chemical reactions, namely nucleophilic additions, cycloaddition reactions, free radical additions, halogenations, hydroxylation, and metal transition complexations, have been reported for C_{60}. However, addition reactions, electron transfer reactions, and reactions involving the opening of the fullerene cage (molecular surgery) have been studied in more detail. It is worth mentioning the ease with which fullerenes are reduced by means of electron-rich chemical reagents as well as electrochemically. Their oxidation, however, is considerably more difficult to achieve. These experimental findings are in agreement with former theoretical calculations which predicted that C_{60} has a low energy LUMO which is triply degenerated and, therefore, accepts up to six electrons in solution to form up to the hexaanion [22]. The theoretical predictions were later confirmed by electrochemical measurements recording from the monoanion to the hexaanion using a toluene/acetonitrile 5:1 by volume solvent mixture at $-10°C$ [23].

For a wider and more detailed study of the basic reactivity of fullerenes, the reader is referred to the aforementioned monographs that comprehensively cover the properties and chemical reactivity of fullerenes [19–21].

2 New Covalent Chemistry of Fullerenes

Significant effort is still being devoted to the chemical modification of fullerenes. Even though most of them are based on the chemistry of electron-poor olefins, fullerene curved double bonds have given rise to a quite peculiar fullerene chemistry. Remarkable examples of this reactivity have been provided by the use of fuller-1,6-enynes, fullerene analogues of 1,6-enynes involving a highly reactive fullerene double bond as the "ene" moiety. Thus, fulleropyrrolidines **1** bearing a propargyl group on the C-2 of the pyrrolidine ring undergo an unusual thermal [2+2] cycloaddition reaction affording regioselectively a cyclobutene-fullerene derivative **2** (Scheme 1) [24]. A different change in chemoselectivity is observed when an internal alkyne is used in the fullerenynes. In that case, allenofullerene derivatives (**3**) are obtained as a result of a formal "ene" reaction where the alkyne moiety with the α CH group acts as an "ene" component, despite the unfavorable geometry (Scheme 1) [25].

Another example of the intriguing behavior of fullerene double bonds has recently been reported by Bazan et al. in which fullerenes behave as a neutral carbon based Lewis acid [26]. Thus, when C_{60} reacts with the N-heterocyclic carbene **4**, that acts as a Lewis base, a thermally stable zwitterionic Lewis acid–base adduct **5** is formed. The bulk of the substituents of carbene species, along with the delocalization of its positive charge, prevent the expected cyclopropanation reaction and a C–C single bond, with a length of 1.506 Å is formed instead (Scheme 2).

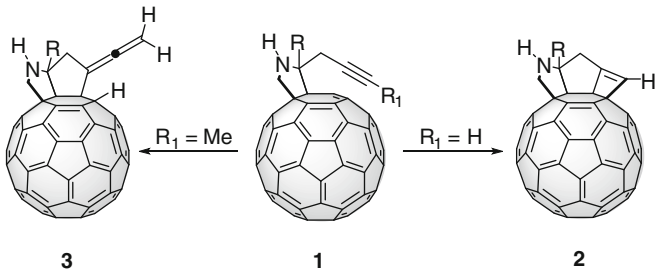

Scheme 1 Fullerenynes (**1**) bearing an alkyne unit give rise to cyclobutene derivatives (**2**) regioselectively, and allenic structures (**3**)

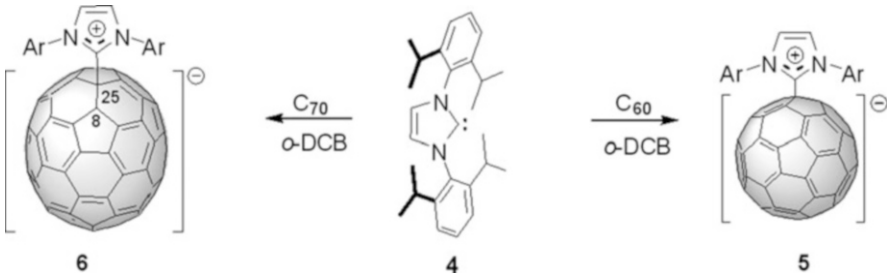

Scheme 2 Fullerene-carbene Lewis acid–base adducts

The addition also occurs onto C_{70} with the regioselective formation of a new bond between the carbene and the carbon atom C-25 of [70]fullerene [27].

Among the numerous methods for chemical functionalization of fullerenes reported during the last decade, some important trends have been outlined for achieving new properties or major control over factors like reactivity, selectivity, and compatibility with a wider range of functional groups.

2.1 New Reactions on Fullerenes Involving Metals

The nucleophilic addition of organometallic reagents, such as organolithium [28] or Grignard salts [29], is one of the classical methods for fullerene functionalization. [30–32]. More recently, the use of transition metals has expanded the arsenal of chemical tools, achieving new structures with better control of reactivity and selectivity. Thus, fullerenes' double bonds, despite their electron-poor character, are able to act as the alkene component in a Pauson–Khand (PK) reaction. Therefore, when a 1,6-fullerenyne is treated with $Co_2(CO)_8$, highly efficient and regioselective intramolecular PK products showing three [33] (or five [34]) fused pentagonal rings on the same hexagon of the fullerene surface were formed (Scheme 3).

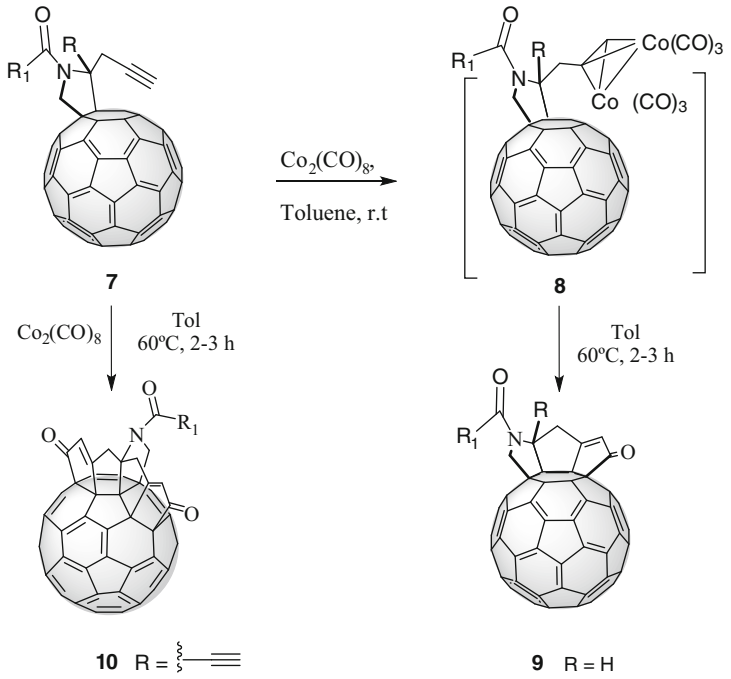

Scheme 3 Pauson–Khand reaction of fullerenynes

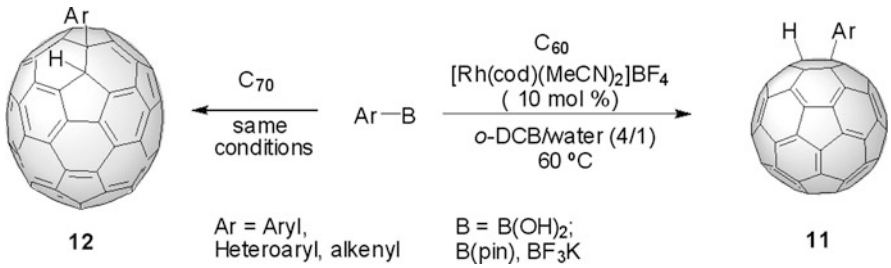

Scheme 4 Rhodium and palladium catalyzed additions of organoborane reagents onto fullerenes

A further step has been the use of transition metal catalysis in fullerene chemistry as a smart alternative to avoid high loading of organometallic reagent and to achieve remarkable levels of reactivity and selectivity. An interesting example of this approach has been the arylation and alkenylation of fullerenes catalyzed by a rhodium complex reported by Itami [35]. Similarly to the reaction of organoboron compounds with electron-deficient alkenes and alkynes, rhodium (I) complexes catalyze the hydroarylation of C_{60} (or C_{70}) with arylboronic acid in aqueous solution. The reaction proceeds with high regioselectivity and in a mono-addition selective manner (Scheme 4)

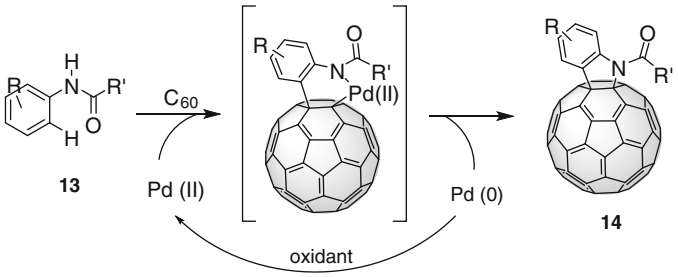

Scheme 5 Fulleroindolines prepared by Pd(II) catalysis

The use of $[Rh(cod)_2]BF_4$ gave rise to an optimal combination of good yield (61%) and excellent selectivity (>95%) showing an important effect of the counteranion of the rhodium complexes in sharp contrast with the reported example of conventional olefins. The authors claimed a catalytic cycle reaction where cationic Rh complex and water produce Rh–OH species. After transmetalation of the thus-formed Rh–OH with $RB(OH)_2$, the Rh–R species undergoes addition on the C_{60} double bond. Finally, protonolysis of the formed fullerenyl Rh species affords the product R–C_{60}–H (**11**, **12**) with regeneration of the cationic Rh species.

Shortly after, the same authors also developed a palladium(II) catalyst Pd(2-PyCH=NPh)$(OCOC_6F_5)_2$ for the hydroarylation of fullerene with boronic acids that, along with good catalytic activity (reaction generally occurs at room temperature), presents a bench stability in the solid state and efficiency under air conditions. Single crystal X-ray diffraction analysis confirmed unequivocally the addition of the aryl moiety and hydrogen in a 1,2-fashion at the α bond of C_{70} with the phenyl group attached at the position close to the pole of the C_{70} unit [36].

Analogously, Co-catalyzed hydroalkylation of C_{60} with reactive alkyl bromides in the presence of Mn reductant and H_2O at ambient temperature gave the monoalkylated C_{60} in good to high yields. The reaction probably occurs through a reduced Co(0 or I) complex that promotes generation of a radical ($R^{\bullet}$) and the addition to C_{60} [37].

An intriguing copper-catalyzed radical reaction that involves a formal C–H bond activation has been reported by Nakamura. The reaction efficiently couples an arylacetylene or enyne to a penta(aryl)[60]fullerene bromide in a formal [4+2] fashion to form a dihydronaphthalene ring fused to a fullerene sphere [38].

Palladium acetate catalyzes cycloaddition onto C_{60} of a variety of anilides through a C–H bond activation, affording fulleroindolines (**14**) in a highly regioselective manner (Scheme 5) [39].

2.2 Asymmetric Catalysis on Fullerenes

Chirality is an important but undeveloped topic in fullerene science [40, 41]. Along with inherently chiral pristine fullerenes, optically active derivatives have been

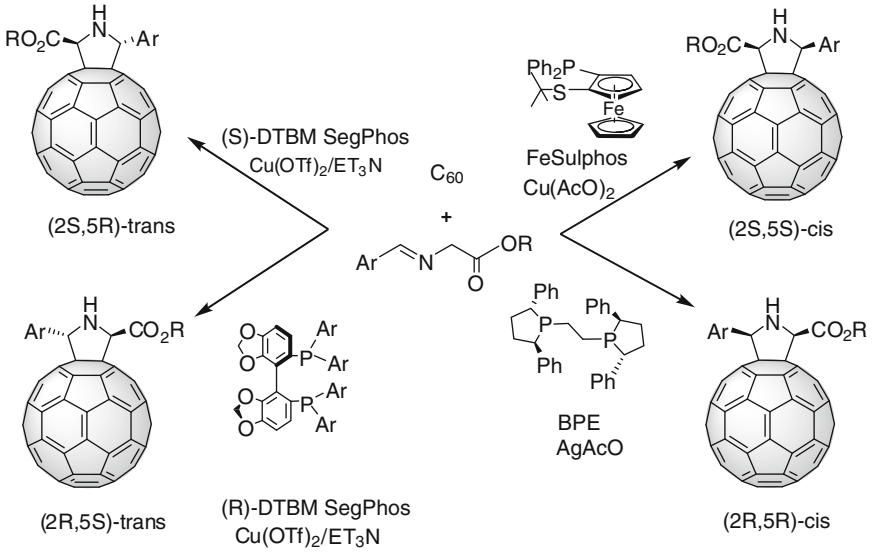

Scheme 6 Stereodivergent 1,3-dipolar cycloaddition of chiral N-metalated azomethine ylides onto C_{60}

obtained by chiral induction from chiral starting reagents or after tedious and expensive HPLC separation from the racemic mixture [40].

The non-coordinating nature of fullerenes has hampered the use of asymmetric metal catalysis and, therefore, the employ of enantiopure fullerene derivatives has been limited to a few examples [42–44].

In this respect, a major breakthrough has been the chiral activation of a 1,3-dipole in the cycloaddition of N-metalated azomethine ylides onto C_{60} (Scheme 6) [45]. By using catalytic amounts of transition metals and the suitable ligand, the cycloaddition of a series of α-iminoesters occurs under very mild conditions and good yields, affording pyrrolidinofullerenes (probably the most important class of fullerene derivatives) with complete control of diastereoselectivity.

More important, chiral complex formed by copper(II) acetate and (*R*)-Fesulphos led the cycloaddition toward the formation of (2*S*,5*S*)-*cis* pyrrolidinofullerenes, whereas the use of silver acetate and chiral (−)-BPE ligand switches the enantioselectivity toward the opposite (2*R*,5*R*)-*cis* pyrrolidinofullerene enantiomers.

Shortly after, complete control on the stereochemical outcome and a fully stereodivergent synthesis of all the possible stereoisomers of disubstituted fulleropyrrolidines was achieved [46]. The use of the complex Cu(II) triflate/(*R*) or (*S*)-DTBM segphos switches the diastereoselectivity towards both enantiomers of the unusual *trans* pyrrolidine with high enantiomeric excess. For this latter process, the authors invoke the presence of a stepwise mechanism that justifies a *supra–antara* formal [4+2] cycloaddition (Scheme 6).

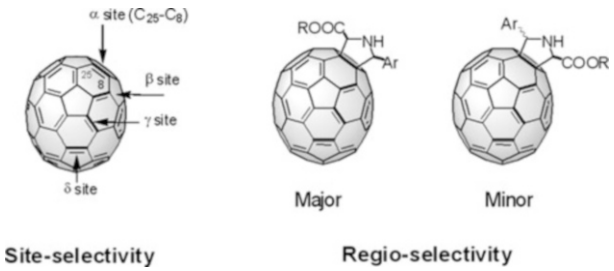

Fig. 4 Site-, regio-, diastereo-, and enantio-selective cycloaddition onto C_{70}

The application of this methodology to higher fullerenes has also been achieved with excellent selectivity. Indeed, higher fullerenes are characterized by a more complex covalent chemistry due to the minor degree of symmetry. In C_{70}, the number of different 6,6 double bonds is increased compared to the single kind of 6,6 double bond in C_{60} and, therefore, even higher control is necessary to face the distinct levels of selectivity encountered.

The very mild conditions used for this transformation allowed direction of cycloaddition of chiral N-metalated azomethine ylides toward the more reactive α double bond (C_{25}–C_8 according IUPAC nomenclature) with an almost complete site-selectivity. Despite the use of unsymmetrical dipoles, all the complexes used afforded the pyrrolidines bearing methoxycarbonyl group in the polar region of C_{70} as major product with good levels of regio-selectivity (Fig. 4) [47].

Finally, for this regioisomer all four possible stereoisomer were obtained by the use of the suitable metal chiral complex with high values of diastereo- and enantio-selectivity [43–45].

Theoretical calculations (B3LYP/LANL2DZ) indicated a stepwise mechanism for this cycloaddition where the first step is critical for the stereochemical outcome. Furthermore, the high regioselectivity has been accounted for by the calculated nucleophilic and electrophilic Fukui indexes.

Chiral functionalization of endofullerenes represents one step further in the application of chiral metal catalysis. The first chiral endohedral metallofullerenes were recently prepared by using such methodology on a racemic mixture of a non-IPR metallofullerene derivative, La@C_{72}($C_6H_3Cl_2$) [48]. This mono-functionalized metallofullerene was chosen due to the calculated energy level of the LUMO orbital being suitable to give rise to 1,3-dipolar cycloaddition. Despite this complexity, eight optically pure bis-adducts of La@C_{72} (four from the clockwise starting material enantiomer and four from the anticlockwise enantiomer) were isolated using non-chiral HPLC. These endohedral fulleropyrrolidines resulted from the addition onto only 2 sites among 108 possible addition sites. For each site, two 2,5-disubstituted pyrrolidine regioisomers are formed with fixed (2*S*,5*S*) and optical purities as high as 98% (Scheme 7). All the isomers feature a strong Cotton effect that is dominated by the inherent chirality of the carbon core. The four isomers

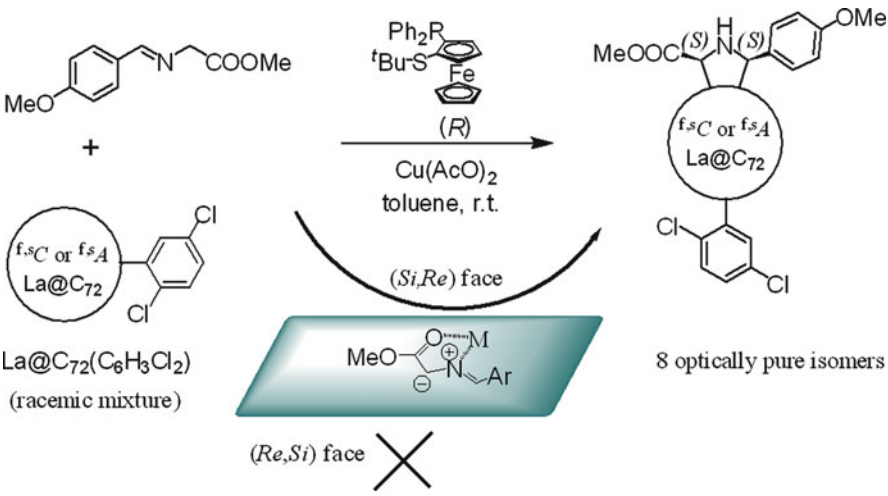

Scheme 7 The 1,3-dipolar cycloaddition reaction of N-metalated azomethine ylide on La@C_{72}($C_6H_3Cl_2$) (as a racemic mixture), using Cu(II) Fesulphos complex as a catalyst, affords eight different optically active pyrrolidines with a fixed (2*S*,5*S*) configuration

formed from the clockwise enantiomers exhibit circular dichroism (CD) spectra that are opposite in sign to those derived from the anticlockwise enantiomer.

2.3 Retro-Cycloaddition Reactions of Fullerene Cycloadducts

Among the many well-known exohedral reactions developed on the fullerene sphere, cycloaddition reactions have played a prominent role with applications in fields such as medicinal chemistry [49] and materials science [50]. The fullerene derivatives obtained through this functionalization method display, in general, an acceptable degree of stability; however, in the last few years a number of studies have reported efficient retro-cycloaddition methodologies for the most important fullerene cycloadducts. In this section we will describe the different retro-cycloaddition conditions for each type of fullerene derivative, and the applications of these methodologies to carry out protection–deprotection protocols that could selectively add or remove addends from fullerenes while leaving others unperturbed.

2.3.1 Retro-Diels–Alder Reaction

Fullerenes are excellent dienophiles that can undergo [4+2] cycloaddition reactions with different dienes such as anthracene or cyclopentadiene. This reaction is controlled by the properties of the dienes and can proceed at room temperature, at reflux or under microwave irradiation. The rate of Diels–Alder reaction is affected

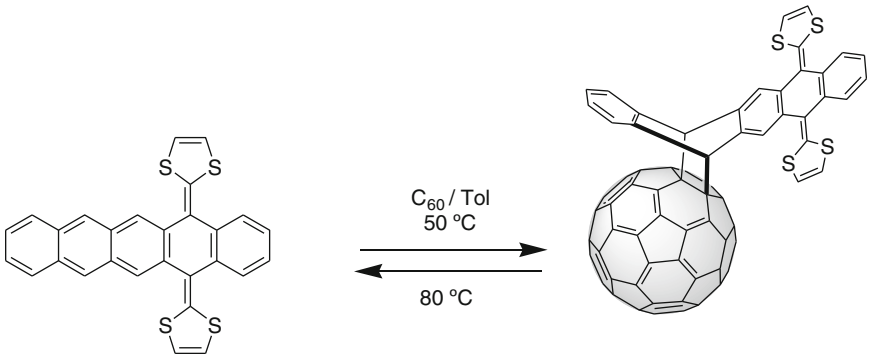

Scheme 8 Thermally reversible C_{60}-based donor–acceptor ensembles

by the overall gain or loss of aromaticity of the dienophile (fullerene core) and/or the diene [51]. Most of these Diels–Alder adducts are thermally unstable and can undergo efficient retro-Diels–Alder upon mild heating [51]. Even though the regiochemistry of Diels–Alder additions is low, a few exceptions have been reported. In this regard, the reaction of C_{60} with an excess of 2,3-dimethyl-1,3-butadiene at elevated temperatures yields a hexakis-adduct with T_h symmetry with an average effective selectivity >80% for each addition step [52].

In our research group we have investigated the Diels–Alder cycloaddition of anthracene derivatives bearing fused π-extended tetrathiafulvalenes (TTFs) to C_{60} to yield thermally reversible donor–acceptor materials (Scheme 8) [53]. NMR and cyclic voltammetry experiments allowed the determination that the retro-cycloaddition process starts around 50°C and continues during the 50–80°C range. Thus, taking advantage of this finding, this donor–acceptor compound is able to act as an ON/OFF switch, using non-fluorescing Diels–Alder adducts of C_{60} which, upon heating, revert to the starting materials.

2.3.2 Retro-Cyclopropanation Reaction

In the Bingel–Hirsch reaction, the deprotonation of an α-halomalonate leads to a nucleophilic anion which attacks the fullerene core to yield methanofullerenes [54]. Using this methodology a large variety of fullerene derivatives have been described and, in general, they are stable in air and under high thermal and oxidative conditions. However, these derivatives can efficiently undergo a retro-cyclopropanation reaction under reduction conditions.

The electrochemical retro-Bingel reaction of the (alkoxycarbonyl)methano-fullerenes of C_{60}, C_{70}, C_{76}, and *ent*-C_{76} at the second reduction potential by controlled potential electrolysis (CPE) has been reported by Echegoyen, Diederich and co-workers [55]. The retro-cyclopropanation by CPE is selective for the methano-addend, which must have at least one strong electron-withdrawing group. The presence of other groups such as cyclohexene, pyrrolidine, and

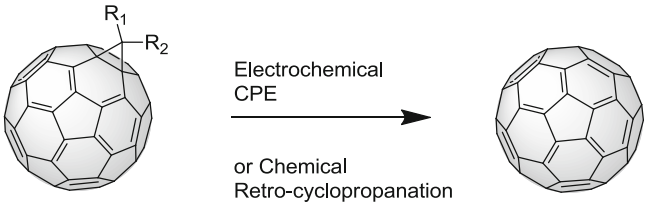

Scheme 9 Different approaches to induce the retro-cyclopropanation reaction

benzocyclobutene rings fused to the [6,6]-bond were not affected by CPE [56]. This singularity offered a new and versatile protecting/deprotecting group strategy. The chemical retro-cyclopropanation of C_{60} and C_{70} mono-adducts was reported in 2000 by Diederich, Echegoyen and co-workers [57]. In this case, the methano-addend was removed from C_{60} and C_{70} after heating at reflux with amalgamated magnesium powder (10% $HgBr_2$) for 3 days, yielding 73% of C_{60} and 63% of C_{70}, respectively. In the case of bis-adducts of C_{60}, the yield of recovered C_{60} varied between 13% and 48% and no isomerization reactions were detected. These chemical conditions can selectively remove only the methano addends in the presence of other functional groups such as pyrrolidines, offering a versatile protecting/deprotecting group strategy (Scheme 9) [57].

2.3.3 Retro-1,3-Dipolar Cycloaddition Reactions

Among the 1,3-dipolar cycloaddition reactions, the addition of azomethine ylides is considered as one of the simplest and most efficient procedures for the functionalization of fullerenes [58]. Azomethine ylides are reactive intermediates that can be generated in several ways, although the decarboxylation of iminium salts, derived from condensation of α-amino acids with aldehydes or ketones, is the easiest and most general procedure commonly followed. Pyrrolidinofullerenes are stable compounds, although in the last few years a number of methodologies have been described to promote the retro-cycloaddition reaction of these derivatives to afford pristine C_{60} fullerene.

Martín et al. [59] have recently described the thermally induced retro-cycloaddition of pyrrolidino[3,4:1,2]fullerenes. The authors studied the retro-cycloaddition process on a series of pyrrolidinofullerenes under a variety of experimental conditions. The best results were obtained heating the corresponding fulleropyrrolidine in the presence of a dipolarophile such as maleic anhydride and copper triflate. Under these conditions, the reaction led to the quantitative formation of the parent unsubstituted C_{60} in all cases. This methodology was also effective in inducing the retrocycloaddition for the mono-adduct mixture of three isomers of [70] fulleropyrrolidine which afforded pristine C_{70} in 95% yield.

Another important finding was the use of C_{60} as a dipolarophile. A mixture of a fullerene bis-adduct was heated to reflux in *o*-DCB in the presence of C_{60} and

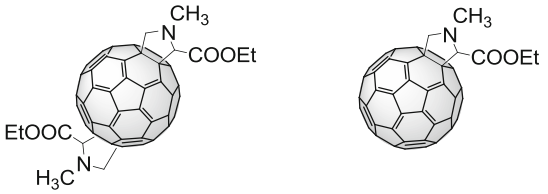

Fig. 5 A mixture of bis-adducts (*left*) in the presence of C_{60} as dipolarophile produces monoadduct (*right*)

HPLC analysis of the reaction confirmed the quantitative formation of the corresponding monoadduct (Fig. 5) [59]. This interesting result opened new avenues for improving the yields of mono-adduct formation from the usually undesired bis-cycloadducts obtained as byproducts in 1,3-dipolar cycloaddition reactions of azomethine ylides to C_{60}. This observation has recently been used as an indirect proof of the covalent attachment of pyrrolidine fragments to single-walled carbon nanotubes (SWCNT). The authors applied the same conditions described by Martín et al. [59] by heating a sample of pyrrolidino-SWCNT in the presence of C_{60} to act as dipolarophile and the corresponding pyrrolidinofullerene compound was detected, thus confirming the efficient trapping of the thermally generated azomethine ylide [60].

Guryanov et al. [61] described an alternative protocol to achieve the retro-cycloaddition of pyrrolidinofullerenes. The authors reported the quantitative retro-cycloaddition of pyrrolidinofullerenes under microwave irradiation in an ionic liquid (1-methyl-3-*n*-octyl-imidazolium tetrafluorborate) without further additives. The combination of microwave irradiation in an ionic liquid offers the unique opportunity for very efficient flash-thermal activation in conjunction with a strong stabilization of ionic intermediates or reactants. In this case, the ionic liquid served as an ideal medium to solvate the incipient 1,3-dipole whose release in solution was likely assisted by electrostatic interactions with the complementary ions of the solvent. In agreement with the mechanism proposed by Filippone et al. [62], cycloreversion occurred through the formation of a reactive 1,3-dipolar intermediate which was expected to be stabilized by the ionic liquid environment.

Lukoyanova et al.[63] had reported an alternative way to induce the retro-cycloaddition of pyrrolidinofullerenes using electrochemical techniques. The authors induce the retro-process by controlled potential electrolysis (CPE) at an applied potential determined from cyclic voltammetry experiments.

In order to determine whether the experimental conditions previously used for the retro-cycloaddition of fulleropyrrolidines and fulleroisoxazolines [64] are suitable for 2-pyrazolinofullerenes, Delgado et al. [65] followed the above-mentioned protocol: excess of dipolarophile, as well as copper triflate to facilitate the retro-cycloaddition process. According to the experimental findings, *C*-aryl-*N*-aryl-2-pyrazolino[60]fullerenes do not undergo an efficient retro-cycloaddition process under a variety of experimental conditions, which reveals that these compounds are thermally stable fullerene derivatives. In contrast, the presence of an alkyl chain in the carbon atom of the pyrazole ring results in an easier cleavage of the 1,3-dipole, leading to pristine C_{60} in good yields (72%). These results show the importance of

thermal stability in order to prepare new C_{60}-based materials, as well as the nature of the substituents (alkyl or aryl) which has a strong influence on the thermal stability of the cycloadducts. In particular, this is a key issue in photovoltaic cells, where long exposure to sunlight results in drastic temperature increases of the photo- and electro-active materials [65].

3 Macromolecular Chemistry of Fullerenes

Soon after the first protocols for the chemical functionalization of fullerene were set up, the rush for its incorporation in polymeric backbones started [66]. The main aim was to combine the well established processability, ease of handling, and toughness of polymers with the rather unique pool of properties of fullerenes in order to achieve new materials with combined features or even with unprecedented properties. Obviously, the final scope of the preparation of such hybrids is their application in cutting edge technologies. Nevertheless, due to the incomplete disclosure of the chemistry of fullerene, the firsts attempts to achieve fullerene-polymers led to uncharacterisable or inutile materials often obtained by employing empirical synthetic methods. Fortunately, these problematics were overcome with the development of well established methodologies for the modification of fullerenes, and nowadays the macromolecular–fullerene hybrids can be designed and tailored at will and fully characterized. Thanks to the synthetic versatility of polymers, several examples of polyfullerenes have been reported to the date, which can be classified accordingly to their chemical structure or to their properties as well as to their applications [67–69]. Herein we use a "classical" classification in which each family is structurally homogeneous and few common protocols can be followed to prepare their corresponding members.

3.1 Classification and Synthetic Strategies

An easy way to order polyfullerenes is accordingly to their increasing chemical complexity and difficulty in preparing them (Fig. 6). The synthesis of macromolecular fullerenes may be as simple as the mixing of C_{60} and a polymeryzing reactant, or may require several carefully controlled reaction steps leading to unprecedented superarchitectures.

Even simpler, in some ways, is the preparation of all-carbon fullerene polymers [70, 71], which are all those materials constituted exclusively by fullerene units covalently linked to each other without any additional linking groups or side groups. The members of this family are prepared by exposing pristine fullerene to a strong external stimulus such as visible light [72], pressure [73], and plasma irradiation [74], with no problems in getting the final structure. During the polymerization, [2+2] cycloaddition reactions between two double bonds of two neighboring C_{60} molecules take place generating new cyclobutane rings [75].

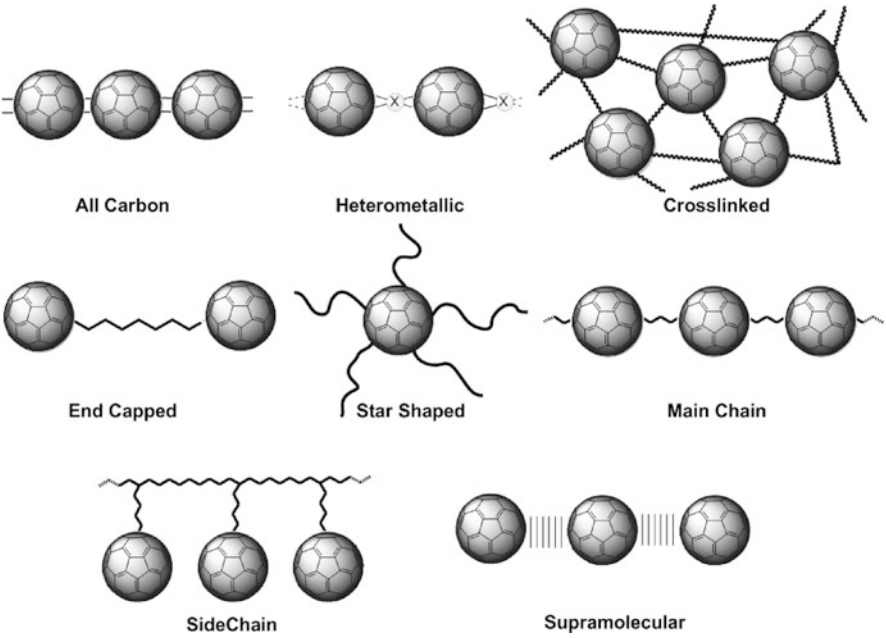

Fig. 6 Structural classification of the different families of C_{60}-polymers

Analogously, heterometallic polymers, a family of heteroatom-containing polymers, in which elements other than carbon are present in their structures, are obtained by means of charge-transfer polymerization mediated by metals [76] and also by electro-reduction in the case of fullerene epoxide [77, 78].

Another family of polyfullerenes that needs little chemical control is the cross-linked set. Their synthesis usually proceeds from tridimensional random and quick reactions involving several of the 30 equivalent double bonds of the fullerene cage. Nevertheless, some control over the addition reactions is required in order to avoid a dramatic intractability of the final products. Different synthetic strategies have been followed till now for their preparation including the reaction between fullerene (or a C_{60}-derivative) and a monomer or with the pending groups (or the end termini) of preformed polymers.

On the other hand, the incorporation of one or two fullerene units at the terminal positions of linear polymeric chains leads to the end-capped C_{60}-polymers. It is worth noting that the presence of C_{60} moieties strongly influences both the molecular and the bulk behavior of the parent polymers as a result of the modification of their hydrophobicity. Two different synthetic strategies have been employed to prepare this class of polymers: the capping of a polymer chain with C_{60} or the growth of a polymeric backbone from the surface of a fullerene moiety or a C_{60}-derivative, the so called "*graft to*" and "*graft from*" approaches. These protocols can also be easily used in the synthesis of the members of the star-shaped polymers, which are constituted by 2–12 long and flexible polymer chains covalently linked to a fullerene cage with topologies similar to that of sea-stars.

One of the less explored families of fullerene polymers is the main-chain one. Here, the C_{60} spheres are directly allocated in the polymer backbone forming a necklace-type structure. Unfortunately, the double addition on the C_{60} moieties results in the formation of complex regioisomeric mixtures (up to eight isomers) and also the formation of cross linking products by multiple additions can occur.

The preparation of these in-chain polymers can be carried out by direct reaction between the C_{60} unit and a suitable symmetrically difunctionalized monomer or by means of polycondensation between a fullerene bisadduct (or a mixture) and a difunctionalized monomer. In contrast, side-chain polymers, sometime called *on-chain* or "*charm-bracelet*," represent the most studied family of polyfullerenes and show the C_{60} pending from the main polymer chain. A century of studies on polymers has been exploited in the binding of C_{60} to all the "classic" families of polymers such as polystyrenes [79, 80], polyacrylates [81, 82], polyethers [83], polycarbonates [84], polysiloxanes [85], and polysaccharides [86] in the search for improved processability and enhanced properties, with a wide range of potential applications. In this family can also be included the "double-cable" polymers [87, 88], in which the π-conjugated semiconducting polymer (p-type cable) with electron-donating characteristics contains electron-accepting fullerene units covalently connected (n-type cable), with remarkable advantages for construction of photovoltaic devices. The synthesis of the members belonging to this family can be achieved by direct introduction of fullerene itself (or a C_{60}-derivative) into a preformed polymer, or by homo-/co-polymerization of a suitable C_{60}-derivative. Moreover, for the double-cable polymers, electropolymerization is also possible.

Finally, the most recent family of macromolecular fullerene is that composed by supramolecular polymers created through any type of self-assembly and via reversible interactions of one or more types of components. Interestingly, these reversible interactions can often allow supramolecular polymers to equilibrate thermally with their monomers or oligomers. There are several ways to obtain such supramolecular assemblies; among them several systems may be obtained by interactions between functionalized polymers and C_{60} derivatives or fullerene itself or through the assembly of self-complementary C_{60} derivatives. More recently, assemblies between ditopic concave guests and [60]fullerene by means of concave–convex complementary interactions have also been reported [89, 90].

3.2 Properties and Applications

Despite hundreds of examples of polyfullerenes having been reported over the last two decades, to date this class of smart material has not had a real application. However, the progress achieved year by year reveals new potential applications and improved properties with respect to early examples, or even with respect to the state of the art, as in the case of photovoltaic applications. In the present section, some of the most promising and recent applications for C_{60}-polymers will be shown. Since 1991 fullerene polymers have been studied as active materials in membranes both for gas separation [91, 92] and for proton exchange fuel cells [93], and also as active

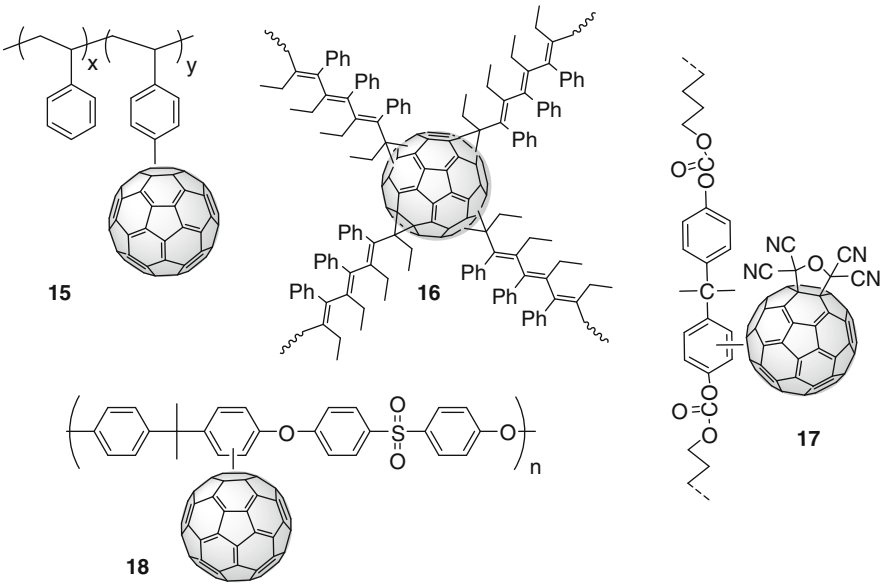

Fig. 7 Chemical structures of polyfullerenes with NLO properties

polymers in electroluminescent devices [77, 94, 95] and in non-volatile flash devices [96], among others. One of the most promising applications for polyfullerenes seems to be as an active layer in optical limiters. These are devices that strongly attenuate optical beams at high intensities while exhibiting higher transmittance at low intensities, which are used for protecting human eyes and optical sensors from intense laser beams. In this regard, C_{60} is an excellent optical limiter operating in a reverse saturable absorption mode [97], and its derivatives may be considered as potent broadband optical limiters due to the broad coverage of the characteristic ground- and excited-state absorptions over a wide wavelength range [98, 99]. However, the poor solubility and processibility of fullerene has limited its use in optical limiting devices and for this reason, in order to overcome such a drawback, C_{60} has been incorporated in polymeric matrices. In Fig. 7 some examples of fullerene-containing polymers used for optical limiting are collected.

In 1995 random solid fullerene-containing polystyrenes (PS) showed nonlinear optical (NLO) properties about five times greater than those of a C_{60} solution [100, 101]. Later on, random poly(methyl methacrylate) [102] and linear PS-containing fullerene **15** (Fig. 7) [103] were found to be optical limiters. In 2000 the star shaped C_{60} containing poly(1-phenyl-1-butyne) **16** turned out to be stable, and film-forming with a fullerene content of up to 9.1 wt%. NLO studies revealed that at 532 nm (Nd:YAG laser) **16** shows improved optical limiting performances compared to C_{60} in solution at a linear transmission of 43% [104]. In the same year the side chain polyfullerene **17**, prepared by Friedel–Crafts addition of C_{60} and of a C_{60}-derivative to a polycarbonate, also displayed good optical limiting properties

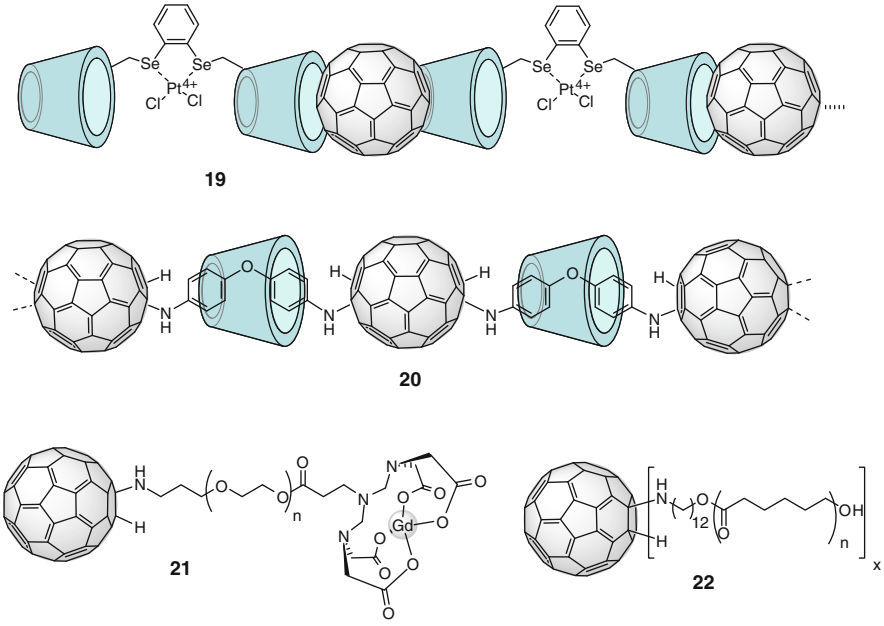

Fig. 8 Structures of DNA-cleaving and fullerene-polymers for PCT

[105]. Interestingly, the polycarbonate endowed with the fullerene derivative behaved better than that functionalized with fullerene itself. Very recently the same synthetic protocol has been used in order to prepare fullerene-functionalized polysulfones **18** [106]. These materials show not only a very high thermal stability and glass transition temperatures depending on the C_{60} content, but also optical limiting properties.

On the other hand, it is well known that fullerene may act as a scavenger. When excited in the ultraviolet region (340–400 nm) it generates reactive oxygen species (ROS) acting as an effective photosensitizer, also useful in the visible-light cleavage of DNA in the photodynamic cancer therapy (PCT) [107]. However, in order to be successfully employed C_{60} needs to be transformed in a water-soluble derivative and, among other things, its incorporation in hydrophilic polymers proved to be an excellent opportunity. In this regard, different polyfullerenes have been tested as DNA cleavers such as the supramolecular polymer **19** [108] formed by fullerene units complexed within the upper rims of cyclodextrin dimers (Fig. 8). Cyclodextrins were also employed in order to afford water solubility to the main chain polymer **20**, formed through nucleophilic polyaddition reaction between C_{60} and the β-cyclodextrin-bis(*p*-aminophenyl) ether [109]. Once again, under visible light conditions **20** proved to be a highly efficient DNA-cleaving agent for oligonucleotides. More recently a photosensitizer with magnetic resonance imaging (MRI) activity has been achieved by linking polyethylene glycol to fullerene at one end and the diethylenetriaminepentaacetic acid Gd^{3+} complex at the other

(**21**, Fig. 8) [110]. Intravenous injection of **21** into tumor bearing mice followed by irradiation showed a significant anti-tumor PCT effect which depended on the timing of light exposure that correlated with tumor accumulation as detected by the enhanced intensity of MRI signals. Finally, the photoactivity of star-shaped poly(ε-caprolactone)-C_{60} **22** has been successfully proven in the benchmark transformation of 9,10-anthracene dipropionic acid into its endoperoxide [111]. In fact, large amounts of $^1O_2$ have been obtained upon irradiation of **22** with visible light. These kinds of polymers are of interest especially because they are biodegradable, biocompatible, and non-toxic to living organisms.

Among the possible practical applications of fullerene-polymers, their use as electron acceptors in the active layer of organic photovoltaic devices seems to be one of the most realistic. Despite the disappointing results, in terms of efficiency, associated with the "double-cable" polymers, investigations of which were time consuming, the very latest few years are witnessing a new momentum in the use of polyfullerenes. This is probably due to improved technologies and methodologies that are allowing scientists to achieve efficiencies comparable to those obtained in bulk heterojunction cells based on molecular C_{60}-derivatives. The first improvement in organic solar cells performances has been obtained by using a new approach in which the glycidol ester of [6,6]-phenyl C_{61}butyric acid has been first prepolymerized in the presence of a Lewis acid as the initiator (**23**, Fig. 9) [112]. Second, after spin coating the prepolymer in a blend with P3HT (poly-3-hexyl thiophene), the ring-opening polymerization has been completed by heating the photovoltaic device which showed 2.0% conversion energy efficiency, probably due to the morphological stabilization of the active layers architecture. Soon after, a new approach was reported in which the amphiphilic diblock-polymer **24** carries both the C_{60} units and P3HT fragments acting as a compatibilizer between PCBM and P3HT in the active layer [113]. When added to a blend of PCBM: P3HT at 17 wt% the photovoltaic device prepared displayed an efficiency of 2.8%, along with enhanced stability of the devices against destructive thermal phase segregation. This improvement has been accounted by for the higher control in the blend morphology of the active layer due to the presence of fragments of P3HT in the polymer backbone which act as compatibilizer between PCBM and P3HT. Analogously, rod-coil block copolymer **25** has been used at various concentrations as surfactant/compatibilizer for the active layer of bulk-heterojunction solar cells in blends with PCBM [114]. This approach resulted in 35% increase of the photocurrent efficiency, increasing from 2.6% to 3.5% when the copolymer was used at 5 wt%. Such enhancement has been ascribed to the improvement in the bicontinuous interpenetrating network due to the compatibilizing action of the copolymer, as also evidenced by AFM studies.

Finally, a revolutionary approach has recently been described in which the cross-linked C_{60}-polymer **26** is generated in situ allowing the subsequent deposition of the active layer to avoid interfacial erosion [115]. The inverted solar cell ITO/ZnO/**26**/P3HT:PCBM/PEDOT:PSS/Ag showed an outstanding device performance with a PCE of 4.4% and an improved cell lifetime with no need for encapsulation. The strength of this new approach is its wide and general application. In fact, changing

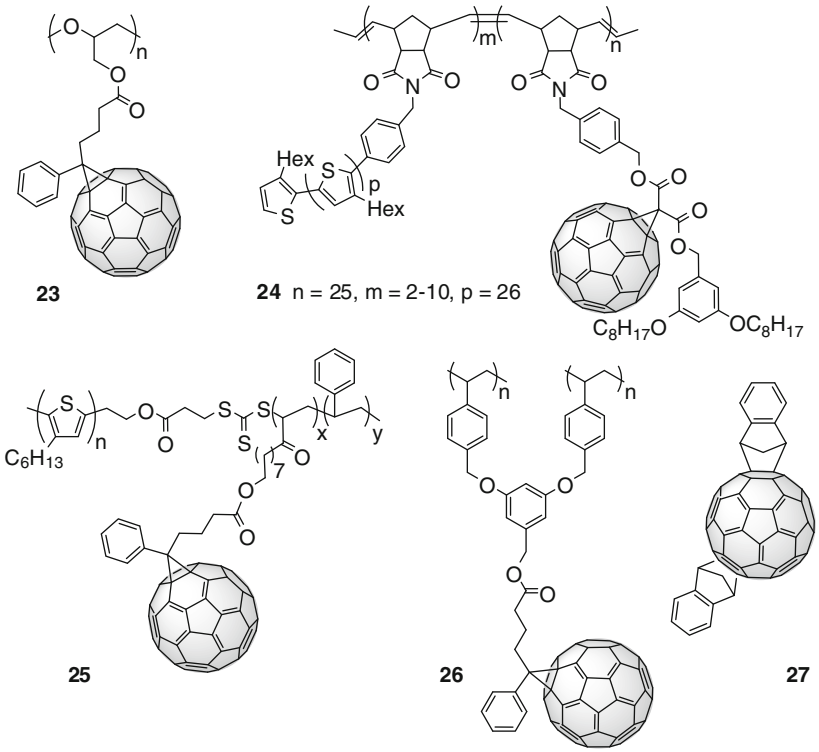

Fig. 9 Fullerene-containing polymers used in organic photovoltaic devices

PCBM with fullerene bis-adduct **27** as acceptor in an inverted bulk heterojunction cell with architecture ITO/ZnO/**26**/P3HT:**27**/PEDOT:PSS/Ag gave rise to the impressive value of 6.22% of efficiency, which retains 87% of the magnitude of its original PCE value after being exposed to ambient conditions for 21 days [116].

4 Supramolecular Chemistry of Fullerenes

The examples of covalent modification of fullerenes we have seen so far imply the saturation of at least one of the double bonds of the polyenic structure. This might be beneficial or detrimental for the application in mind. Alternatively, the chemist can choose to interact with the fullerenes or their derivatives in a supramolecular fashion, making use of weak noncovalent interactions. In the following we will very briefly review some of the most important advances in H-bonded fullerene assemblies as well as the host–guest chemistry of fullerenes, organized according to the main type of noncovalent interaction present in the associates.

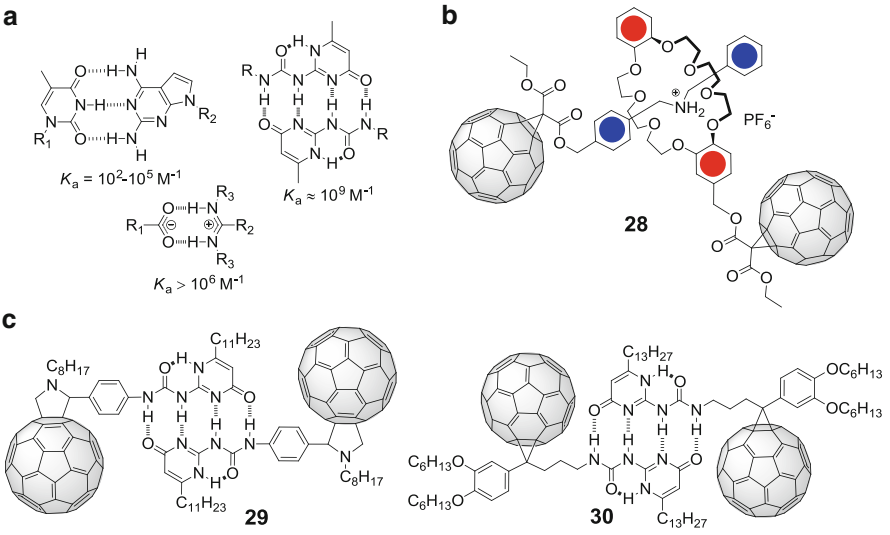

Fig. 10 (**a**) Illustration of different H-bonded supramolecular architectures. (**b**) First C_{60}-based supramolecular dimer. (**c**) Chemical structures of supramolecular dimers of C_{60}

4.1 H-Bonded Fullerene Assemblies

H-bonds are, perhaps, the best studied non-covalent interactions. Although they are weak interactions, with binding energies in the range of ~ 5 kcal/mol, hydrogen bonds are also selective and directional [117]. When molecules interact by forming two or more hydrogen bonds, secondary electrostatic interactions can give rise to dramatic differences in the stability of the supramolecular complexes. The combination of different non-covalent interactions, such as ionic, π–π interactions, etc., with hydrogen bonds allows one to modulate the affinity between the interacting molecules, giving rise to a wide spread of supramolecular architectures (Fig. 10).

The importance of hydrogen bonds in determining the geometry and, overall, the function of biomolecules such as DNA, RNA, proteins, tobacco mosaic virus, and so forth is well known. Another natural example comes from the photosynthetic apparatus, in which a highly ordered supramolecular array of electron-donors (chlorophylls) and electron-acceptors (quinones) harvests and converts sunlight into chemical potential energy through cascades of short-range electron transfer steps [118]. Inspired by the natural photosynthetic event, intramolecular photoinduced electron transfer processes have been thoroughly studied in different covalent and non-covalent systems formed by donor and acceptor electroactive moieties for their implementation in molecular electronic devices [119, 120]. In this context, fullerene C_{60} has probably been the most studied electroactive entity owing to its unique electron-acceptor properties and low reorganization energy in electron transfer processes.

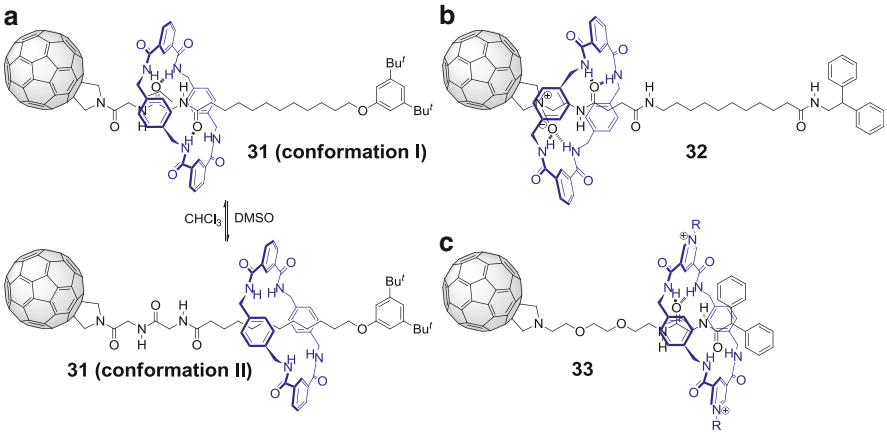

Fig. 11 (**a**) Solvent switchable rotaxane. (**b**) Stabilization of an N-oxide fulleropyrrolidine by encapsulation in the rotaxane. (**c**) Electrochemically driven molecular shuttle

The first example of a supramolecular H-bonded architecture involving fullerene was a dimer with a pseudorotaxane-type structure (**28**, Fig. 10) reported by Diederich et al. [121]. For this dimer a K_a value of ~970 M^{-1} was obtained. More robust supramolecular dimers of fullerene were obtained by employing a quadruple array of H-bonds based on 2-ureido-4-pyrimidone (UP) (**29** and **30**) [122, 123]. In these cases the DDAA H-bonds disposition gives rise to complementary pairs with affinities in the range of $K_a \sim 10^6$ M^{-1}.

Leigh-type clipping reactions have allowed the preparation of several fullerene containing rotaxanes. The first bistable rotaxane containing a fullerene is depicted in Fig. 11 (**31**) [124]. Depending on the polarity of the solvent, the macrocycle resides preferentially over the glycylglicyne unit or over the alkyl chain. A slight modification of the structure of the thread allows the macrocycle to shuttle in the opposite direction, from the amide to the fullerene moiety [125].

This displacement of the macrocycle has been used to increase the stability of a fulleropyrrolidine N-oxide (**32**, Fig. 11) [126]. The formation of hydrogen bonds between the macrocycle and the N-oxide inhibits the deoxygenation reaction, thus enhancing the stability of the N-oxide derivative.

Remarkably, the shuttling of the macrocycle can also be stimulated electrochemically by the formation of the fullerene trianion [127]. This electrochemically driven molecular shuttling has recently been achieved at very low reduction potential by introducing positive charges in the macrocycle (**33**, Fig. 11). In the latter case, only one electron is needed to induce the operation of the shuttle [128].

The first reported donor–acceptor supramolecular dyad based on C_{60} is a pseudorotaxane formed between the dibenzylammonium salt of a Bingel-type fullerene and the crown ether of a zinc phthalocyanine (**34**) [129]. This complex has an association constant of ~ 1.4×10^4 M^{-1} and, what is more important, an

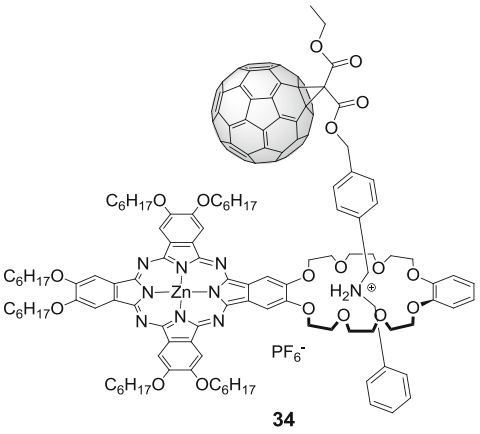

Fig. 12 First fullerene containing supramolecular donor–acceptor dyad

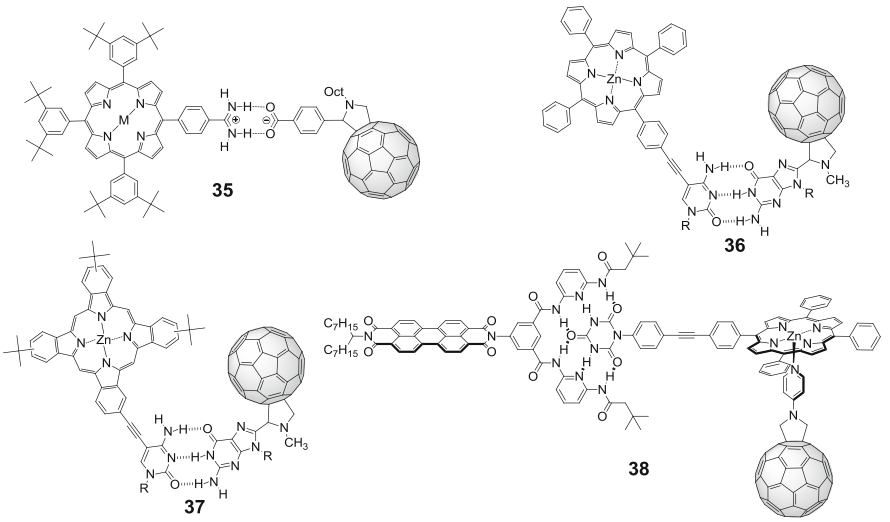

Fig. 13 Donor–acceptor dyads with different H-bonding motifs

intracomplex photoinduced electron transfer process leads to a radical pair species ($C_{60}^{\bullet -}$–$ZnPc^{\bullet +}$) with a remarkable lifetime in the region of microseconds (Fig. 12).

Since that, a plethora of donor–acceptor dyads in which the acceptor unit is a fullerene C_{60} have been studied. These studies have revealed that a strong electronic communication is found through the supramolecular ensembles. That is the case for dyad **35** (Fig. 13) [130], formed by a two point amidinium–carboxylate bonding motif which gives rise to an extraordinarily high affinity, with a K_a value up to 10^7 M^{-1} in toluene. The strong electronic coupling (36 cm^{-1}) facilitates the formation of a long-lived radical pair with a lifetime of ~1 μs in THF.

Dyads **36** and **37** employ a three point guanosine–cytidine couple to form fullerene based hybrids with a porphyrin or phthalocyanine respectively. While

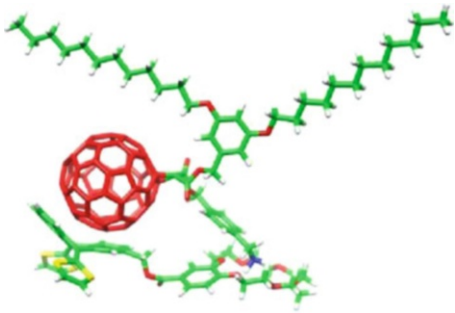

Fig. 14 Molecular model of exTTF-crown ether/fullerene ammonium salt complex

for the first dyad the formation of a charge separated state after irradiation with a long lifetime of ~2.02 μs was observed, the lifetime of the radical pair in the case of the zinc phthalocyanine dyad was only 3 ns [131, 132]. This difference has been ascribable to a pronounced coupling between the ZnPc and C_{60} in **37**, which is reflected in a large binding constant of 1.7×10^7 M^{-1} (vs a K_a of 5.1×10^4 M^{-1} found for **36**).

The six-point Hamilton array has also been used to form highly stable dyads when interacting with a cyanuric acid moiety, with association constants usually in the range of 10^4–10^5 M^{-1} for monotopic receptors [133] and even higher when a ditopic Hamilton receptor is employed [134]. In recent work, Hirsch et al. have employed this Hamilton receptor together with metal complexation to control the step-by-step assembly of the different components in triad **38** [135]. In this triad the perylenediimide (PDI) moiety acts as a light harvester unit and, after selective photoexcitation, an energy transfer to the porphyrin unit takes place, which has been corroborated by steady-state and time-resolved measurements. The energy transfer is followed by an electron transfer event from the porphyrin to the axially complexated fullerene moiety driving to the formation of a radical ion pair with a lifetime of 3.8 ns. This lifetime is longer than that of the corresponding dyad from the porphyrin and the fullerene.

Tetrathiafulvalene (TTF) and π-extended tetrathiafulvalene (exTTF) have also been used as the electron donor counterpart in D–A nanohybrids with fullerenes in supramolecular assemblies. In pseudorotaxane-type structures between exTTF and C_{60}, it has been found that the interaction between the donor moiety of exTTF and the acceptor unit of fullerene is stronger when a flexible spacer allows the involvement of the intramolecular interaction between the convex fullerene surface and the concave face of exTTF (Fig. 14) [136]. In this case, a binding constant of 1.58×10^6 M^{-1} in chlorobenzene was observed, more than two orders of magnitude higher than the K_a values obtained for related systems in which only the crown ether-ammonium salt motif can interact. For this dyad a remarkable anodic shift of ~ 100 mV of the oxidation potential of exTTF reflects the strong donor–acceptor interaction. Transient absorption spectroscopy showed the formation of a radical ion pair with a lifetime of 9.3 ps.

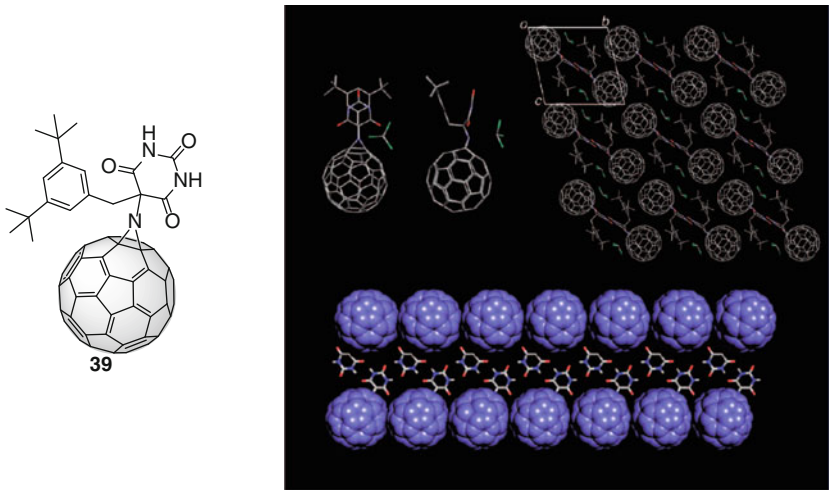

Fig. 15 Chemical structure and solid-state crystal structure of hydrogen-bonding barbiturate fullerene **39** highlighting the close van der Waals contacts between fullerenes in the H-bonding ribbon. (Reprinted with permission from [137]. Copyright 2010 American Chemical Society.)

An appealing topic in molecular electronics is the use of supramolecular interactions to control the assembly of the electron donors and acceptors in order to obtain highly ordered supramolecular entities with specific functions. In this context, Bassani et al. reported the hierarchical self-assembly of a barbituric acid appended fullerene and a thiophene oligomer substituted with a melamine moiety to build a photovoltaic device. They found that the photocurrent is 2.5-fold greater in this device than in analogous ones constructed with fullerene C_{60} and the oligomer without the H-bonding units, which is attributable to higher order at the molecular level [137].

Recently, trying to take advantage of the ability of supramolecular assembly to control the electronic interactions between the fullerene units, OFET devices were constructed with derivative **39**, which combines the solubilizing 3,4-ditertbutylbenzene group with the barbituric acid motif [138]. The fabricated OFET devices showed a mobility approximately two orders of magnitude lower than the devices constructed with pristine fullerene, owing to the anisotropy of the electrical conductivity of the crystals of **39** (Fig. 15).

4.2 On Concave–Convex Interactions

We have just seen some examples of supramolecular associates of fullerene derivatives based on hydrogen bonding. All of these rely on the previous covalent modification of the fullerene to introduce adequate chemical groups. Pristine fullerenes, on the other hand, are unfunctionalized, approximately spherical polyenes. From the point of view of their supramolecular chemistry this means

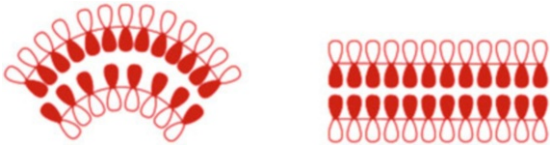

Fig. 16 Scheme depicting the concave–convex interaction vs planar π−π interaction

that very weak, non-directional dispersion interactions (mainly van der Waals and π−π) will account for the vast majority of the binding energy in host–guest complexes [139]. Since these forces depend directly on surface area, the shape complementarity between host and guest becomes critical. In this sense, distorted concave recognition motifs seem ideally suited for the association of the convex fullerenes. The importance of this shape complementarity is beautifully illustrated by the distortion from planarity observed in the solid state structure of some porphyrin–fullerene supramolecular complexes reported by Aida. In the associates the porphyrins adopt a non-planar concave conformation to maximize the positive interactions with the C_{60} guest, even at the expense of some degree of conjugation [140]. Besides the optimization of dispersion interactions due to shape complementarity between concave hosts and convex fullerene guests, in 2006 Kawase and Kurata suggested that there might be an additional positive effect arising from the unsymmetrical nature of the π orbitals of the contorted molecules with respect to the convex (outer in the case of the fullerenes) and concave (inner in the case of the fullerene) sides [141]. They termed this "concave–convex interaction" (Fig. 16).

Despite this, most of the examples of receptors for fullerene reported to date rely on planar recognition motifs. Curved molecules are geometrically tensioned structures, with bond angles away from the preferred ones and consequently are not always an easy synthetic target. However, some concave molecules are synthetically accessible and have been employed as hosts for fullerenes. We will now overview some prominent examples.

Corannulene consists of five benzene rings fused into a central five-member ring. As could be expected considering its size – nearly identical to that of C_{60} and thus too small to associate with it – chemical derivatization is necessary to enlarge the cavity of corannulene and observe binding. Following this strategy, several monotopic receptors have been reported [142].

A ditopic receptor, "buckycatcher" **40**, was synthesized by Sygula et al. joining together two units of coronene via a rigid aromatic spacer [143], forming a tweezers-like host [144]. It forms stable complexes with C_{60} (log $K_a = 3.9$, d_8-toluene, room temperature),[1] in which the fullerene is included between the two coronene units, as demonstrated through X-ray diffraction studies on cocrystals of **40** and C_{60} (Fig. 17).

Another very interesting family of curved aromatic hosts for fullerenes are the cyclic [*n*]*para*-phenyl acetylenes (CPPAs, **41**–**44** in Fig. 18) reported by Kawase

[1] All through the article we will report binding constants as logarithms, and without an error interval, for simplicity. The reader can refer to the original publications for these data.

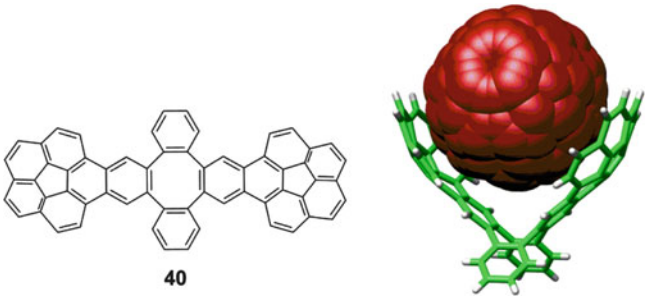

Fig. 17 Chemical structure of the "buckycatcher" and solid state structure of its complex with C_{60}. Note that the fullerene unit is disordered in the crystal. Reprinted with permission from [144]

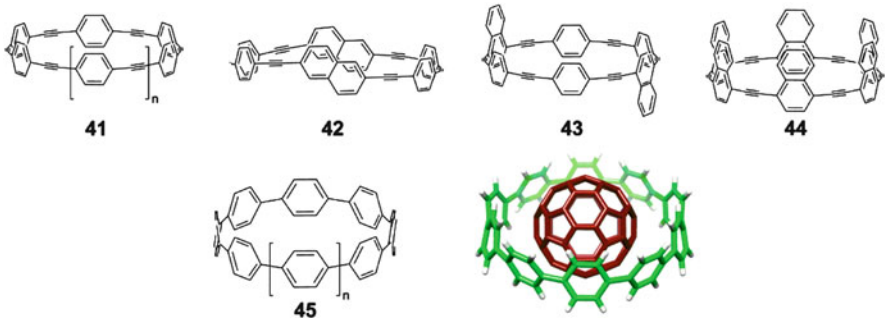

Fig. 18 Chemical structure of some CPPAs and general structure of CPPs. The solid state structure of the [10]CPP·C_{60} associate is also shown

et al. in 1996 [145]. The diameter of the cavity of **41** is 1.33 nm as found in its solid state structure, a close to perfect fit for C_{60}. Consequently, the ability of **41** to associate with [60] fullerene was investigated through UV–vis titrations, the analysis of which afforded a binding constant of log $K_a = 4.2$ in benzene at room temperature [146]. In order to increase the depth of the cavity, and in turn increase interactions between host and fullerene, macrocycles **42**–**44** (Fig. 18) were synthesized [147]. In these carbon nanorings at least two of the *p*-phenylene moieties are substituted by naphthalene units. This structural optimization bore fruit, as all of the newly synthesized hosts form complexes of remarkable stability with both C_{60} and C_{70}. In fact, the binding constants in benzene were log $K_a > 5$ as estimated through fluorescence quenching experiments.

Cycloparaphenylenes (CPPs, **45** in Fig. 18), in which the phenyl units are connected directly, have also been synthesized [148], and their association with fullerenes investigated. In particular, [10]CPP presents a concave cavity of 1.34 nm in diameter, ideally suited to associate with C_{60}. Indeed, it does so with a remarkable association constant of log $K_a = 6.4$ in toluene at room temperature [149]. These experiments have been followed up by the group of Jasti, who have reported

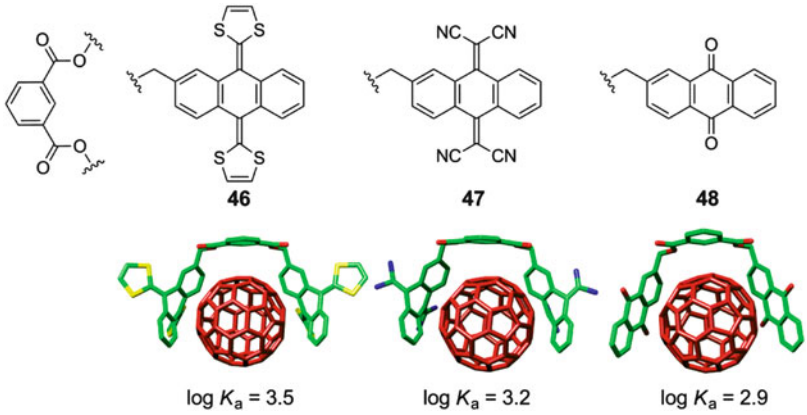

Fig. 19 Chemical structure of receptors **46–48** and molecular models of their complexes calculated at the BH&H/6-31 G** level

the synthesis of gram quantities of [8]- and [10]cycloparaphenylenes, and the crystal structure of the [10]CPP·C_{60} complex [150].

We have reported extensively on the ability of the curved electron donor exTTF to serve as a recognition motif for fullerenes. The geometric and electronic complementarity between the concave aromatic face of exTTF and the convex surface of the C_{60} was exploited to build very simple tweezers-like receptors (**46**, in Fig. 19) which associate with C_{60} with respectable binding constants in the order of log K_a = 3–4, in several solvents at room temperature [151, 152]. Thanks to their synthetic accessibility we could access a collection of hosts in which we could investigate the specific contribution of concave–convex interactions to the molecular recognition of C_{60} (**46–48** in Fig. 19) [153]. All three receptors bear the same number of aromatic rings and are approximately equal in size, so the contribution of π−π and dispersion interactions can be considered equivalent. Hosts **46** and **47** both feature concave recognition motifs, and differ only in their electronic character: while the exTTF moiety in **46** is an electron donor, the TCAQ units in **47** are electron acceptors. Meanwhile, the anthraquinone fragments in **48** have a similar electronic character to **47**, but are completely flat. Unsurprisingly, **46** shows the highest association constant, due to the combination of electronic and geometric complementarity towards C_{60}. Remarkably, there is a noticeable difference between the binding affinities of **47** and **48** that can be attributed to concave–convex interactions. As we noted in our original communication, whether concave–convex interactions should be treated as a new kind of intermolecular force or just a particular case of preorganization is not straightforward. In any case, it is worth considering them for the few curved guests of interest, mainly fullerenes and carbon nanotubes [154].

We have also investigated the binding abilities of π-extended derivatives of tetrathiafulvalene with a truxene core (truxTTF), which feature up to three dithiole units connected covalently to the conjugated aromatic core. To accommodate the

dithioles, the truxene moiety breaks down its planar structure and adopts an all-*cis* sphere-like geometry with the three dithiole rings protruding. The concave shape adopted by the truxene core perfectly mirrors the convex surface of fullerenes, indicating that van der Waals and concave–convex π−π interactions between them should be maximized. Indeed, the association of trux-TTF and fullerenes in solution was investigated by ^{1}H NMR titrations with C_{60} and C_{70} as guests affording binding constants of log $K_a = 3.1$ and 3.9 for C_{60} and C_{70} in $CDCl_3/CS_2$, respectively [155].

4.3 Tweezers and Macrocycles for the Molecular Recognition of Fullerenes

As we have seen in some of the examples described above, tweezer-like hosts have been a particularly popular design for the construction of receptors for fullerenes. This is so because tweezers are usually synthetically accessible, since it requires only connecting two recognizing units symmetrically via a spacer.

One of the earliest examples of molecular tweezers for C_{60} was reported by the group of Fukazawa in 1998 [156]. They connected two units of calix[5]arene through a variety of rigid spacers, and obtained the best results for host **49**, which showed a binding constant of log $K_a = 4.9$ in toluene at room temperature, a world record in complex stability at the time.

The positive interaction between porphyrins and fullerenes has often been exploited to construct this kind of receptor [157]. The first example of such porphyrin tweezers for fullerenes was reported by Boyd, Reed and co-workers over a decade ago [158]. They connected two porphyrin units appended with pyridine ligands through coordination of palladium. The structure of the tweezers **50** is shown in Fig. 20. The binding constant of this receptor towards C_{60} was estimated to be log $K_a = 3.7$ in toluene-d_8 at room temperature.

After this first example the same authors reported very similar receptors, in which the coordination link between the porphyrin units was substituted with covalent bonding through the amides of either isophthalic or terephthalic acid [159]. This resulted in a decrease in the association constant. Later, in collaboration with the group of Armaroli, they replaced the benzenedicarboxamide spacers with several calixarenes, reaching binding constants as high as log $K_a = 5.4$ and 6.4 for C_{60} and C_{70} respectively, both in toluene at room temperature [160].

A more sophisticated example of molecular tweezers for C_{60} (**51** in Fig. 21), with a mechanism to turn "on" and "off" their ability to bind the fullerene guest, was reported by Shinkai and co-workers [161]. As synthesized, each of the appending pyridines coordinates to the porphyrin metal, keeping the two porphyrins on opposite sides and preventing association of C_{60}. When an external palladium center is added, the conformation changes to bring both porphyrins to the same side of the molecule, allowing for association with fullerene, as shown in Fig. 21. In the

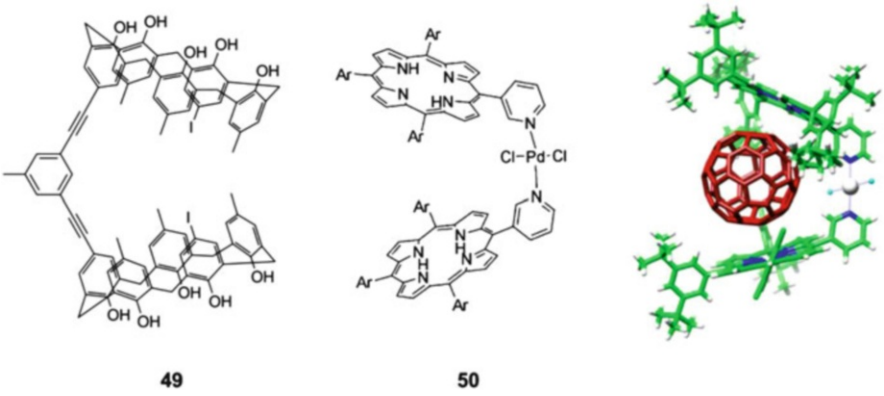

Fig. 20 Chemical structure of the biscalix[5]arene host **49** [157], the "jaws" receptor **50** [158], and X-ray crystal structure of the **50**·C_{60} complex

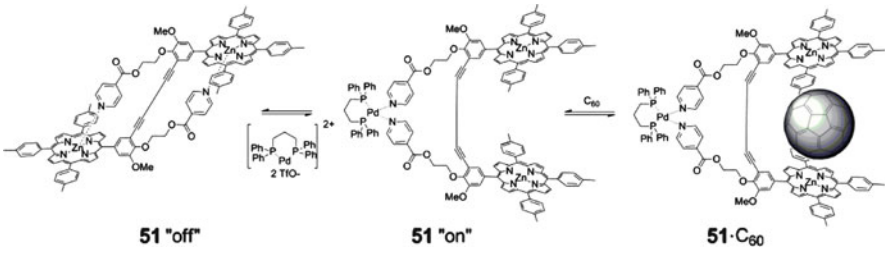

Fig. 21 Structure of the switchable receptor **51** and scheme showing its switching between the "off" and "on" states and its binding to C_{60}

"on" state, the binding constant was estimated to be log $K_a = 3.7$ in toluene/CH_2Cl_2 (50:1) at room temperature.

A distinctive advantage of the simplicity of the tweezers-like design is that it can easily be adapted to construct more elaborate supramolecular assemblies at relatively low synthetic cost. For instance, in our group, based on the exTTF tweezers **46**, we have built both linear [162] and hyperbranched [163] supramolecular polymers [164], covalent dendrimers capable of associating several units of C_{60} [165], and have extended the design to associate with and solubilize carbon nanotubes in aqueous solution.

On the negative side, tweezers are not well preorganized unless very rigid spacers are used to link the two recognizing units. This results in relatively modest association constants, in the case of fullerenes typically in the order of 10^3–10^4 M^{-1}. To obtain complexes of higher stability, a tried and tested strategy is to move from tweezers to macrocycles. Macrocycles are much better preorganized, and have better expressed binding sites, increasing the binding constants significantly. In return, they are more challenging synthetic targets, and the cavity of the host needs to be fine-tuned to match the size of the guest, or the preorganization will

	Z	R_1	R_2	R_3	M_1	M_2
52a	$-(CH_2)_6-$	Hex	Hex	H	Zn(II)	Zn(II)
52b	$-CH_2-C\equiv C-C\equiv C-CH_2-$	Hex	Hex	H	Zn(II)	Zn(II)
52c	$-(CH_2)_6-$	Me	Hex	H	Ir(III)	Ir(III)
52d	$-(CH_2)_6-$	H	H	*t*Bu	Me, H	Rh(III)

Fig. 22 Structure of the macrocyclic bisporphyrin receptors reported by Aida

actually be detrimental to the binding event [166]. We will now see a few examples of macrocyclic hosts for fullerenes to illustrate these points.

In 1999, Aida, Saigo and co-workers published the first example of a bisporphyrin macrocyclic host for C_{60} (**52a** in Fig. 22) [167], initiating what would become one of the largest and most successful families of receptors for fullerenes [140]. Through multiple structural variations they have been able to establish some clear structure–binding affinity relationships. For instance, it has become apparent that not only the length but also the flexibility of the links between the porphyrins is critical to the association event. The synthetic precursors to the alkane spacers are the corresponding alkynes, **52b**. The macrocycles with these rigid spacers do not show *any* sign of binding towards C_{60}, despite theoretically having a cavity of the right size. In contrast, the macrocycles with flexible alkane spacers show remarkably high binding constants, including the world-record in complex stability, **52c**, with an incredibly high log $K_a = 8.1$ toward C_{60} in 1,2-dichlorobenzene (*o*-DCB) at room temperature [168]. This is a dramatic example of the price one has to pay for increased preorganization: it is often a make or break situation.

In the last few years, examples of macrocyclic hosts for fullerenes including more than one porphyrin recognition motif have been reported. Anderson's group has described a rigid cyclic porphyrin trimer, **53**, which associates with C_{60} with log $K_a = 6.2$ [169]. The cavity of **53** is actually better suited to host higher

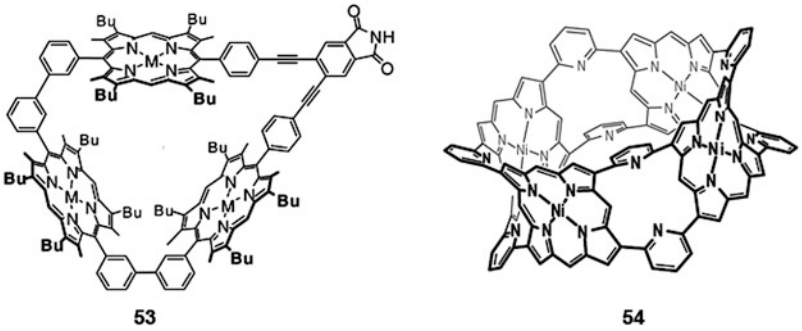

Fig. 23 Structures of the cyclic porphyrin trimer **53** and of nanobarrel **54**

fullerenes, so it shows a binding constant of log $K_a = 8.2$ for C_{70} and log $K_a > 9$ for C_{86}, all in toluene at room temperature.

Osuka and co-workers have gone one step further, linking four porphyrin units to form what they called a "nanobarrel" (**54** in Fig. 23) [170]. The solid state structure of **54** shows a rigid concave cavity of adequate size to associate with C_{60}. Despite this, the authors reported a binding constant of log $K_a = 5.7$ in toluene at room temperature, perhaps not as large as could be anticipated. This might be due to the use of Ni porphyrins, since previous studies have shown a decrease in the binding constant of approximately one order of magnitude from zinc to nickel in macrocyclic porphyrin dimers [171]. Alternatively it might be that the very rigid structure of **54** is not sufficiently flexible to optimize the C_{60}-porphyrin distances, again showing the adverse effects of an excess of preorganization.

Our group has also gone the distance from tweezers to macrocycles. We have recently synthesized a family of nine macrocyclic exTTF-based receptors, in which we have conserved the basic features of the tweezers design (two exTTF units linked through an aromatic spacer) and added alkene-terminated alkyl spacers, to perform ring-closing metathesis [172, 173]. We produced systematic variations of both the aromatic and the alkyl spacers, as shown in Fig. 24. The structural variation strategy proved to be successful, as among the family of hosts we found some of the best purely organic hosts for both C_{60} and C_{70}. For instance, *p*-xylmac12 associates with C_{60} with log $K_a = 6.5$ in chlorobenzene and 7.5 in benzonitrile, both at room temperature. Perhaps more interestingly, the synthesis of such a complete family of macrocyclic receptors showed that even very small variations in structure can lead to huge changes in binding abilities. For example, there is a difference of three orders of magnitude between the association constant of *p*-xylmac12 towards C_{60} and that of *p*-xylmac10 (log $K_a = 3.5$ under the same experimental conditions). Besides changes in the stability constants, we even found variations in the stoichiometry of the associates. The smaller members of the family, *p*-xylmac10 and *m*-xylmac10, associate with C_{70} forming both 1:1 and 2:1 host:guest complexes, while naphmac10, with only a slightly bigger cavity, forms exclusively 1:1 associates.

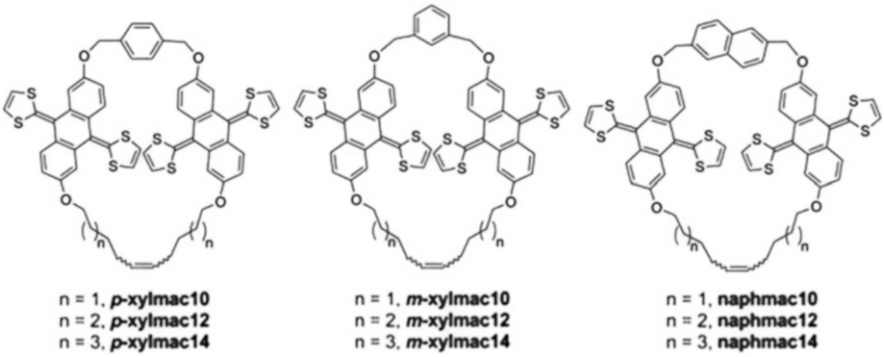

Fig. 24 Chemical structure of the exTTF-based macrocyclic hosts. Reprinted with permission from [173]

There are many other examples of tweezer-like and macrocyclic hosts for fullerenes, which we will not discuss in this chapter. The interested reader can refer to more comprehensive reviews [144, 166]. In this very brief account we intended to outline general considerations regarding the design principles for the construction of hosts for fullerenes, illustrating them with a few selected examples.

5 Endohedral Fullerenes: Improving Size, Shape, and Electronic Properties

Almost immediately after the discovery of the fullerene family, scientists wondered about the possibility of introducing different atoms and molecules into the carbon cages and speculated about the new properties that the hybrid materials could exhibit. This expectation, far from decreasing, is actually growing with the application of these materials in different fields such as medicine or molecular electronics [174]. The properties of endohedral fullerenes can easily be modified depending upon the species entrapped and the fullerene cages. In this sense, endohedral fullerenes are classified in two principal categories:

1. *Metallofullerenes*, which are those that contain elemental metals or their combined forms [175]. More specifically, this family includes *classical metallofullerenes*, $M@C_{2n}$ or $M_2@C_{2n}$, with $60 \leq 2n \leq 88$ [176], *metallic carbides*, $M_2C_2@C_{2n}$ and $M_3C_2@C_{2n}$, where $68 \leq 2n \leq 92$ [177], *metallic nitrides*, $M_3N@C_{2n}$, with $68 \leq 2n \leq 96$ [178], and, more recently, *metallic oxides*, $M_4O_2@C_{80}$ [179]. These fullerenes are typically produced by laser-vaporization or arc discharge techniques of graphite-metal oxides composite materials in the atmosphere of certain gases [180].

2. *Fullerenes encapsulating small molecules*, such as noble gas atoms (helium, neon, argon, krypton, and even xenon have been introduced inside fullerene cages), which are obtained by treating the fullerene powder under forced conditions (650°C

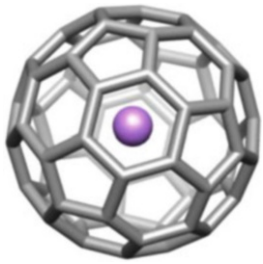

Fig. 25 Drawing for the cationic metallofullerene $Li^+@C_{60}$

and 3,000 atm of noble gas), although the occupation level of the guest is as low as 0.1–1% [181]. In a second approach, molecules as water have been introduced in C_{60} and C_{70} cages by using organic reactions in the so-called "molecular surgery" [182]. This strategy consists in a series of steps which involve making an incision in the fullerene cage to form an opening on the surface, inserting the desired molecule through the opening, and finally closing the hole to reproduce the fullerene cage while retaining the guest species.

The case of $H_2O@C_{60}$ is quite remarkable, since single-crystal X-ray analysis of the complex $[H_2O@C_{60}{\cdot}(NiOEP)_2]$ (OEP = octaethylporphyrin) reveals that, in contrast to many metallofullerenes where the metal often adopts an off-center location and does not move freely, the O atom is located at the center of C_{60}, with the O–H bonds pointing towards the Ni atoms. In addition, $H_2O@C_{60}$ and the empty fullerene can be separated quite easily by HPLC on a pyrenylated stationary phase, in stark contrast to the case of noble gas atoms or H_2 endohedrals. This easy access to a non-hydrogen-bonded H_2O molecule inside the apolar fullerene cage allows the investigation of the properties of the isolated H_2O molecule as well as the modification of the exohedral chemical reactivity of a unique *wet* C_{60}.

From the two categories of endohedral fullerenes mentioned above, the electronic properties of metallofullerenes are particularly promising considering that they are featured by a charge transfer from the encapsulated metal atoms to the carbon cage, forming a non-dissociating salt that consists of metal cation(s) encapsulated in a fulleride anion [183]. This electron-transfer was regarded to stabilize not only the encapsulated species but also the fullerene cage that can sometimes be otherwise unstable in the empty form. A striking example of this ionic model was the isolation of the cationic endohedral metallofullerene $Li^+@C_{60}$ (Fig. 25) [184], which can only be stabilized significantly in ambient conditions when it co-exists with an appropriate counteranion. For example, the crystal structure of the salt $[Li^+@C_{60}](PF_6)^-$ exhibits a strong interaction between Li^+, residing inside the C_{60} cage, and PF_6^- on the outside, the interaction being shown to occur through the six-membered rings [185].

In the following sections we are going to concentrate on mono- and divalent metallofullerenes and metallic nitrides, since these metallofullerenes have been extensively investigated and their chemical reactivity reasonably explored.

5.1 Metallofullerenes and TNT Endofullerenes

Smalley and co-workers demonstrated in 1991 that a family of lanthanum containing fullerenes were produced under a modified Krätschmer–Huffman reactor and that extraction with toluene yielded mostly La@C_{82} (Fig. 26), which was the first endohedral fullerene to be isolated [186]. La@C_{82} has an electronic state best described as $[La]^{3+}[C_{82}]^{3-}$ with an open-shell electronic structure that is a consequence of a three-electron transfer from lanthanum to C_{82} [187]. The resulting electron spin of La@C_{82} imposes a unique chemical reactivity comparable to radical species, inducing magnetism on the molecular scale, or an enhanced electron conductivity [188, 189].

Since the isolation and characterization of the first mono-endohedral metallofullerene, La@C_{82}, many other classical M@C_{2n} (M = Sc, Y, La, Ce, Gd, etc.) have been obtained, with a C_{2v}-C_{82} most abundant cage [176]. In all these fullerene cages filled with a single metal, the metal is not in the center of the cage but tends to coordinate with the cage carbons, being situated under a hexagonal ring along the C_2 axis. As a result, the distribution of charge density is highly anisotropic over the surface, with electrophiles and nucleophiles selectively attacking the two different regions [190].

In the case of the endohedral fullerenes containing two metal, the M_2@C_{80} (M = La, Ce, etc.) cage is typically obtained, with the two isomers I_h and D_{5h} as the most abundant [176]. In the case of these endohedral metallofullerenes, not only is the metal–cage interaction important but also the metal–metal interaction is crucial for the positioning and moving of the metal atoms. In the case of M_2@I_h-C_{80} structures, it has been demonstrated how the metal atoms circulate three-dimensionally [191], in contrast to M_2@D_{5h}-C_{80} species, where the metallic atoms circulate two-dimensionally along a band of ten contiguous hexagons inside the D_{5h}-C_{80} cage [192].

However, for a long period of time the development of the chemistry of endohedral metallofullerenes was impeded by the relatively low yields in which they were produced. An important breakthrough in this chemistry occurred in 1999, when Dorn and co-workers reported the production of trimetallic nitride clusters with high yields [193]. In the trimetallic nitride template (TNT) method, packed graphite rods (metal oxide/carbon/catalyst) are burned in the presence of a dynamic flow of He/N_2 and afforded macroscopic quantities of materials such as Sc_3N@C_{80}, with yields that exceed those of the third most abundant (next to C_{60} and C_{70}) empty cage C_{84}, produced under normal conditions.

The isolation of Sc_3N@C_{80} in macroscopic quantities has facilitated the study of its physical structure and chemical reactivity [180]. From the seven possible constitutional isomers for C_{80} satisfying the isolated pentagon rule (IPR), interestingly only the two least stable empty isomers with I_h and D_{5h} symmetries are the ones that predominate when they are filled with metallic nitride clusters, the I_h isomer certainly being the most abundant [194]. When considering the electronic structure of I_h-C_{80} it is possible to rationalize this observation. It is characterized by

Fig. 26 Molecular structures of La@C_{2v}-C_{82}, La_2@I_h-C_{80}, and Gd_3N@I_h-C_{80}

the presence of an energetically low-lying fourfold degenerate LUMO, which enables this fullerene to accept up to six electrons, and the electronic distribution may be represented by the ionic model: $(Sc_3N)^{6+}@(C_{80})^{6-}$ [195].

Considering the TNT method, endohedrals of the type $M_3N@I_h$-C_{80} have been prepared for very different metals (M = Sc, Y, La, Ce, Nd, Gd, Tb, Dy, Ho, Er, etc.) and, in general, the metal cluster rotates freely inside the fullerene, with the M_3N unit adopting a planar geometry, except for the case of $Gd_3N@I_h$-C_{80} (Fig. 26), where the nitride ion is out of the plane of the three gadolinium ions [196].

Upon increasing the size of the encapsulated metal, the yield of cluster fullerenes usually decreases, and a distribution of molecules is obtained with larger metal ions favoring larger cages. For example, with gadolinium six cages are formed: $Gd_3N@C_{78}$, $Gd_3N@C_{80}$, $Gd_3N@C_{82}$, $Gd_3N@C_{84}$, $Gd_3N@C_{86}$, and $Gd_3N@C_{88}$ [197], whereas for the larger lanthanum only the formation of three very large cages, $La_3N@C_{88}$, $La_3N@C_{92}$, and $La_3N@C_{96}$, is observed [198]. In addition, Echegoyen and co-workers found a remarkable influence of the cage structure on the electrochemistry of the $Gd_3N@C_{2n}$ family [197]. The cage size does not seem to affect significantly the reduction potential of these compounds, which displayed very similar first reduction potentials, but the oxidation potentials shift from +0.58 V vs Fc^+/Fc in $Gd_3N@C_{80}$ to +0.06 V vs Fc^+/Fc in $Gd_3N@C_{88}$, which suggests that the HOMO of the TNT-endofullerenes is probably cage-centered.

5.2 Chemical Reactivity of Endohedral Fullerenes

The chemical functionalization of endohedral metallofullerenes is essential to generate materials easy to process for multiple potential applications. Initial experiments on the functionalization of endohedral fullerenes demonstrated a high reactivity and the formation of multiple adducts or regioisomeric mixtures [199]. However, a remarkable regioselectivity has been observed in a few cases depending on the encapsulated cluster, metal species, carbon cage size or symmetry.

More specifically, the I_h isomer of the C_{80} carbon cage presents high symmetry, with only two possible [1,2] addition sites: bonds between two hexagonal rings

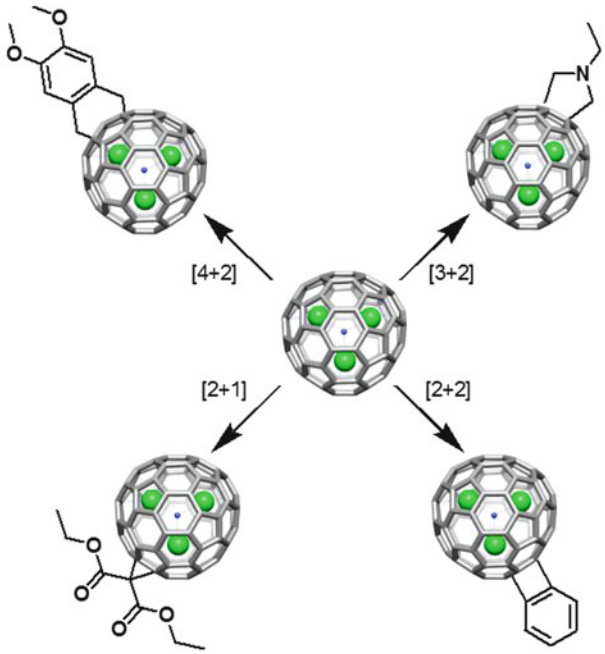

Fig. 27 Representative examples of cycloaddition monoadducts obtained by chemical reaction with Sc_3N-I_h@C_{80}

([6,6]-junctions) and those between pentagonal and hexagonal rings ([5,6]-junctions) [200]. Several reactions have already been reported considering these C_{80} cages: carbene additions [201], radical trifluoromethylations [202], or free radical additions [203], even though cycloaddition reactions are the most effective way to generate covalent derivatives of endohedral metallofullerenes to date.

[4+2]Cycloadditions. The Diels–Alder monoadduct resulting from heating an excess of 6,7-dimethoxyisochroman-3-one and $Sc_3N@C_{80}$ in trichlorobenzene (Fig. 27) was the first isolated organic derivative of a TNT endofullerene [204]. NMR experiments served to identify the regioisomer obtained as the one localized in a [5,6] ring junction of the I_h isomer, which was later corroborated by solving the X-ray structure of the Diels–Alder monoadduct [205]. TNT endofullerenes have a much lower reactivity than empty fullerenes and classical endohedral metallofullerenes and Dorn and co-workers used this selective reactivity to purify TNT endohedral metallofullerenes directly from as-prepared soots in a single facile step in Diels–Alder reactions with a cyclopentadiene-functionalized resin [206].

[3+2]Cycloadditions. So far these have been the processes more intensively investigated, in particular 1,3-dipolar cycloaddition reactions of azomethyne ylides to yield fulleropyrrolidines (Fig. 27) [200, 207], disilirane additions [208], and more recently cycloadditions with epoxides such as tetracyanoethylene oxide [209], or azides to form azafulleroids after nitrogen extrusion [210].

Disilirane additions were used to control the motion of the encapsulated Ce atoms inside the C_{80} cage of $Ce_2@C_{80}$. In this compound, the free random motion of two Ce atoms is regulated under a hexagonal ring on the equator by the electron donation from the silyl groups, exohedrically introduced, to the C_{80} cage [211]. The motion of La atoms encapsulated inside fullerenes has also been controlled exohedrically, by the addition positions, in pyrrolidine adducts of $La_2@C_{80}$. Two different compounds are obtained: in the [5,6]-adduct the two La atoms rotate rather freely, whereas in the [6,6]-adduct the metallic atoms are in fixed positions inside the cage [212].

The regioselectivity of 1,3-dipolar cycloaddition reactions of in situ generated azomethine ylides can also be controlled by the trimetallic nitride cluster. In this sense, Echegoyen et al. demonstrated that when the fullerene inner metal cluster was Sc_3N, the only product detected was the adduct at a [5,6]-junction (product of thermodynamic control). On the other hand, the 1,3-dipolar cycloaddition reaction occurred initially at a [6,6]-junction for the $Y_3N@C_{80}$, and underwent rearrangement to the thermodynamically more stable $Y_3N@C_{80}$ [5,6]-monoadducts upon heating [213]. These experimental results, as well as the computational studies by Poblet and Echegoyen, seem to indicate that, after thermalization of the kinetically favored product, a pirouette-kind of mechanism gives rise to the [5,6]-monoadduct that is thermodynamically preferred [214]. The rate of this rearrangement depends on the internal cluster and on the pyrrolidine addend.

Pyrrolidine adducts have been used as the organic addend to connect electron-acceptor $Sc_3N@C_{80}$, $Y_3N@C_{80}$, or $La_2@C_{80}$ units to powerful donors such as ferrocene [215] or π-extended tetrathiafulvalene derivatives (exTTFs) [216] in the preparation of electron–donor–acceptor (D–A) systems that, upon photoexcitation, yield radical ion pair states with remarkable lifetimes.

[2+2]Cycloadditions. The reaction of benzyne, generated from isoamyl nitrite and anthranilic acid, with $Sc_3N@I_h$-C_{80} was successfully carried out recently to afford both [5,6]- and [6,6]-monoadducts (Fig. 27) [217]. Interestingly, when the reaction was carried out with 2-amino-4,5-diisopropoxybenzoic acid instead of anthranilic acid and under an aerobic atmosphere, in addition to the expected [2+2] benzyne adducts, oxygenation of the [5,6] regioisomer produces an intriguing third product, which is an open-cage metallofullerene. Under an inert atmosphere, the reaction gave only the expected [2+2] adducts [218].

[2+1]Cycloadditions. The investigation of the Bingel reaction on endohedral metallofullerenes demonstrates the remarkable regioselective control exerted by the encapsulated species. The [2+1] cycloaddition of bromodiethylmalonate (the Bingel–Hirsch reaction) in the presence of the non-nucleophilic base 1,8-diazabicyclo[5.4.0]-undec-7-ene (DBU) produced extremely stable derivatives with $Y_3N@C_{80}$ and $Er_3N@C_{80}$ [219], while $Sc_3N@C_{80}$ did not react under the same experimental conditions. Under these conditions, the cyclopropanation of $Sc_3N@C_{78}$ with diethyl bromomalonate produced only one monoadduct and one dominant symmetric bisadduct. The high regioselectivity in the second addition is supported by the highest LUMO surface electron density value for the reactive bond, which corresponds to the kinetically preferred site for a second nucleophilic attack [220].

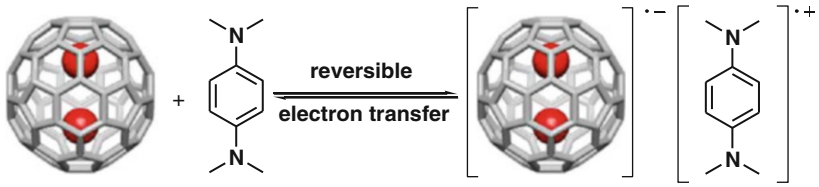

Fig. 28 Intermolecular complexation and electron transfer behavior between $La_2@C_{80}$ and the organic donor molecules TMPD

Another useful [2+1] cycloaddition process is the addition of diazocompounds, generated in situ from tosylhydrazones in basic media, to fullerenes. This reaction has been used for the preparation of relevant endohedral metallofullerene adducts in the context of organic photovoltaics, such as endohedral metallofullerene ($Sc_3N@C_{80}$, $Lu_3N@C_{80}$, or $Ce_2@C_{80}$) PCBM-based derivatives [221] or the first D–A dyad where an endohedral metallofullerene, $Lu_3N@C_{80}$, acts as an electron donor upon photoexcitation. In particular, when connected to perylenebisimide units [222].

Electrosynthetic routes have also been recently explored for the preparation of endohedral metallofullerene adducts that might not be accessible by conventional synthetic routes. In this sense, the different nucleophilicity observed by TNT dianions [223] and trianions [224] seems to be particularly relevant for the preparation of $Sc_3@C_{80}$ derivatives.

Surprisingly, the non-covalent functionalization of endohedral fullerenes has been scarcely investigated, only a few examples about the complexation with calixarenes and crown or thiacrown ethers are known, and size matching was found to be critical to the stability of the resulting complexes [176]. The most promising example is the formation of stable radical ion pairs of *N*-substituted *p*-phenylenediamine with $La@C_{82}$ and $La_2@C_{80}$ [188, 225]. Such spin-site exchange processes are reversible in solution and are readily controllable by changing the temperature and the solvent (Fig. 28).

6 Fullerenes for Organic Electronics

As mentioned above, a huge number of fullerene derivatives have been prepared, many of which have been tested in so-called organic molecular electronics. Their remarkable electron-accepting ability and low reorganization energy combined with solubility in organic solvents and outstanding photophysical properties have made fullerenes a most appealing system to be used in the preparation of electronic devices such as organic photovoltaics and the study of molecular wires, which are discussed in detail in the following sections.

6.1 Fullerenes for Organic Photovoltaics

Global dependence on fossil fuels is a key issue with important consequences in the world today. A reasonable alternative to overcome this need is the use of renewable energy sources, like solar energy, which could, in principle, fulfil our energy requirements with environmentally clean procedures and low prices. Actually, the energy received from the Sun, calculated to be 120,000 TW (5% ultraviolet, 43% visible, and 52% infrared), surpasses by several thousandfold that consumed by the planet. [226].

Photovoltaic (PV) solar cells are currently a hot topic in science and since the original silicon-based device was prepared by Chapin in 1954 exhibiting an efficiency around 6% [227], different semiconducting materials (inorganic, organic, molecular, polymeric, hybrids, quantum dots, etc.) have been used for transforming sunlight into chemical energy. Among them, photo- and electro-active organic materials are promising due to key advantages such as the possibility of processing directly from solution, thus affording lighter, cheaper, and flexible all-organic PV devices. The most widely used configuration of polymer solar cells is based on the use of a fullerene derivative as the acceptor component. Indeed, fullerenes have been demonstrated to be the ideal acceptor because of their singular electronic and geometrical properties and the ability of their chemically functionalized derivatives to form a bicontinuous phase network with π-conjugated polymers acting as electron conducting (n type) material (Fig. 29).

A great variety of chemically modified fullerenes were initially synthesized for blending with semiconducting polymers and to prepare photovoltaic devices. These fullerene derivatives were covalently linked to different chemical species such as electron acceptors, electron donors, π-conjugated oligomers, etc. [119] (Fig. 30). However, in general, the obtained blends resulted in PV devices exhibiting low energy conversion efficiencies [228].

The best known and most widely used fullerene derivative as acceptor for PV devices is [6,6]-phenyl-C_{61} butyric acid methyl ester (PCBM, **55**) [229]. Since its first reported application in solar cells [230], it has been by far the most widely used fullerene, being considered as a benchmark material for testing new devices. This initial report inspired the synthesis of many other PCBM analogues [231] in an attempt to increase the efficiencies of the cells by improving the stability or PV parameters such as the open circuit voltage (V_{oc}) by raising the LUMO energies of the fullerene acceptor.

In this regard, only small shifts (<100 meV) of the LUMO level have been obtained by attaching a single substituent on the fullerene sphere, even by using electron-donating groups. In contrast, significantly higher V_{oc} values have been achieved through the polyaddition of organic addends to the fullerene cage (~100 mV raising the LUMO per saturated double bond). Recently, an externally verified power-conversion efficiency of 4.5% has been reported by Hummelen et al. employing a regioisomeric mixture of PCBM bisadducts as a result of an enhanced open-circuit voltage, while maintaining a high short-circuit current (J_{sc}) and fill factor (FF) values [232].

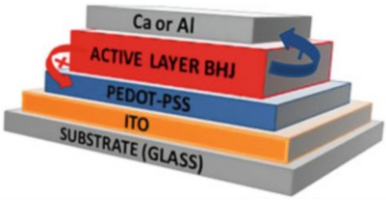

Fig. 29 Typical sandwich-like architecture for a (OPV) solar cell. Polymers and fullerene derivatives are bended on the active layer

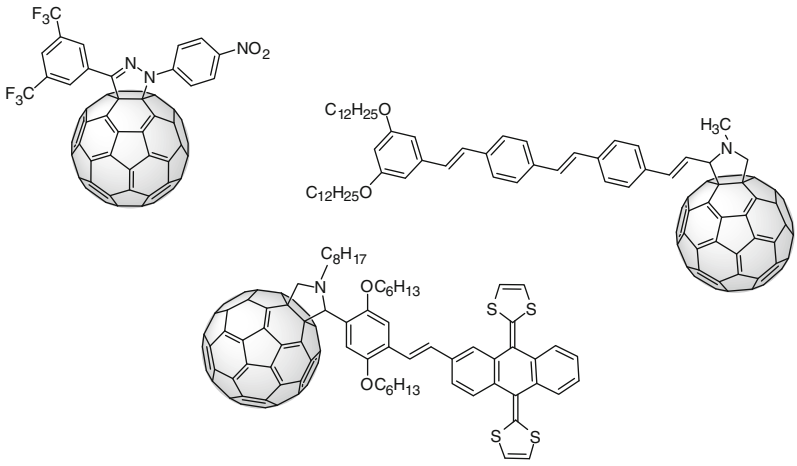

Fig. 30 Some examples of modified fullerenes bearing different organic addends used to prepare photovoltaic devices

The cyclopropanation reaction to superior fullerenes to form PCBM analogues is more complex than for C_{60}. Indeed, the less symmetry and the presence of more than one reactive double bond are often responsible for the formation of regioisomeric mixtures. Nevertheless, the loss of symmetry of C_{70} induces a stronger absorption, even in the visible region. As a result, $PC_{71}BM$ [233] is considered a suitable candidate for more efficient polymer solar devices. Moreover, such devices displayed the highest verified efficiency determined so far in a BHJ solar cell, with an internal quantum efficiency approaching 100% [234]. Analogously, $PC_{84}BM$ [235] has been obtained as a mixture of three major isomers. The stronger electron affinity and the diminished solubility gave rise, however, to poor power conversion efficiencies.

Although the PCBMs are the acceptors that guarantee best performances, it does not mean that they are necessarily the optimum fullerene derivatives. Therefore, a variety of other fullerene derivatives [236] have been synthesized in order to improve the device efficiency or to achieve a better understanding of the dependence of the cell parameters on the structure of the acceptor.

One of the most promising modified fullerene prepared so far is the diphenylmethanofullerene (DPM12, **56**) prepared by Martín et al. [237] endowed with two

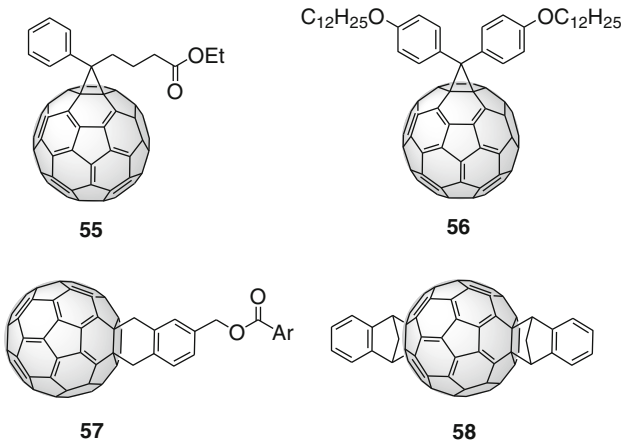

Fig. 31 PCBM (**55**), DPM-12 (**56**) and other modified fullerenes used as successful acceptors for photovoltaic devices

alkyl chains which improve dramatically the solubility of the acceptor in the blend to reach efficiencies in the region of 3% (Fig. 31). Although the LUMO energy level for DPM12 is the same as that for PCBM, an increase in the V_{oc} of 100 mV for the DPM12 over PCBM has been observed [238]. This is currently an important issue for improving the design of future fullerene-based acceptors.

Other fullerene derivatives such as the dihydronaphthylfullerene benzyl alcohol benzoic ester (**57**) described by Fréchet et al. [239] have also shown their ability to produce efficient PV devices (PCE up to 4.5%).

Hou and Li reported the preparation of a bis-adduct fullerene derivative **58** formed by two indene units covalently connected to the C_{60} sphere [240]. Interestingly, the presence of two aryl groups improves the visible absorption compared to the parent PCBM, as well as its solubility (>90 mg/mL in chloroform) and the LUMO energy level, which is 0.17 eV higher than PCBM. Photovoltaic devices formed with P3HT as semiconducting polymer revealed PCE values of 5.44% under illumination of AM1.5, 100 mW/cm^2, thus surpassing PCBM which afforded an efficiency of 3.88% under the same experimental conditions.

Although some of the fullerene derivatives prepared to date exhibit outstanding performances in PV devices, the synthesis of new fullerene derivatives with stronger visible and NIR absorption and higher LUMO energy levels than PCBM is currently a challenge in organic photovoltaics.

6.2 Fullerenes for Molecular Wires

Donor–bridge–acceptor (DBA) systems, in which the bridge mediates the transport of charge between the donor and the acceptor, provide good models to study the

electron transfer processes at the molecular level. In these systems the rate of charge transfer (CT) is a combination of a strongly distance-dependent tunneling mechanism (or superexchange) and a weakly distance-dependent incoherent transport (or hopping).

The attenuation factor, β, is the parameter usually employed to describe the quality of a system as molecular wire, so that the lower the β value the longer the distance that the charge can be moved efficiently. The β parameter is characteristic for the decay of CT rate constant, k_{ET}, as a function of distance, R_{DA}:

$$k_{ET} = k_0 \, e^{-\beta R_{DA}}$$

Typical β values can vary from 1.0–1.4 $Å^{-1}$ for proteins to 0.001–0.06 $Å^{-1}$ for highly conjugated bridges [241]. Other parameters exert an impact on the rate of charge transfer, in particular the underlying driving forces ($-\Delta G^{\circ}$), the corresponding reorganization energies (λ), and the electronic couplings (V) between the donor and acceptor moieties. Therefore β value depends not only on the bridge but rather on the wire system as a whole, that is, the DBA system, whether the D and A termini are molecular units or metallic contacts.

The unique electronic properties of fullerenes have prompted the study of the molecular wire behavior of different molecular bridges connected to fullerene C_{60} as the electron acceptor and different electron donor fragments [242, 243]. The study of these systems with various bridge lengths allows the measurement of distance-dependent charge separation (CS) and charge recombination (CR) rates and, therefore, the determination of the corresponding β values.

It is well documented that molecular wires that exhibit *para*-conjugation facilitate charges to be transferred over larger distances and hence show lower β values related to non-conjugated bridges. Very fast electron transfer for both CS and CR has been reported for compound **59**, with two acetylene bonds connecting the C_{60} unit with the β-position of ZnP ($k_{CS} > 1 \times 10^{11}\ s^{-1}$, $k_{CR} = 2.5 \times 10^{10}\ s^{-1}$) [244]. In contrast, for compounds **60**, in which the polyacetylene bridge is connected through a phenyl ring in the meso position of the porphyrin, CS and CR are in the regions of $7.5 \pm 2.4 \times 10^{9}\ s^{-1}$ and $1.6 \pm 0.2 \times 10^{6}\ s^{-1}$, with a β value of 0.06 $Å^{-1}$ in PhCN [245]. This difference in the rate of electron transfer is due, at least in part, to more favorable orbital interactions between ZnP and C_{60} in **59** and suggests that the phenyl ring retards the electron transfer processes (Fig. 32).

When comparing these systems with a ZnP–*p*-phenylenebutadiynilenes–C_{60} series (**61**), the k_{CS} and k_{CR} values decrease drastically as the distances increase from 22 to 40 Å (k_{CS} range from $1.0 \times 10^{10}\ s^{-1}$ to $1.1 \times 10^{8}\ s^{-1}$ and k_{CR} range from $2.1 \times 10^{6}\ s^{-1}$ to $4.6 \times 10^{5}\ s^{-1}$) giving a quite large attenuation factor of 0.25 $Å^{-1}$ in PhCN [246]. This β value suggests that the phenyl ring inserted in the polyalkyne bridge acts as a resistor for electron transfer, giving rise to a less effective superexchange mechanism.

For the β-substituted ZnP–oligophenyleneethynylene–C_{60} systems **62** (ZnP–oPPE–C_{60}), a strong increase in the lifetime of the charge separated state

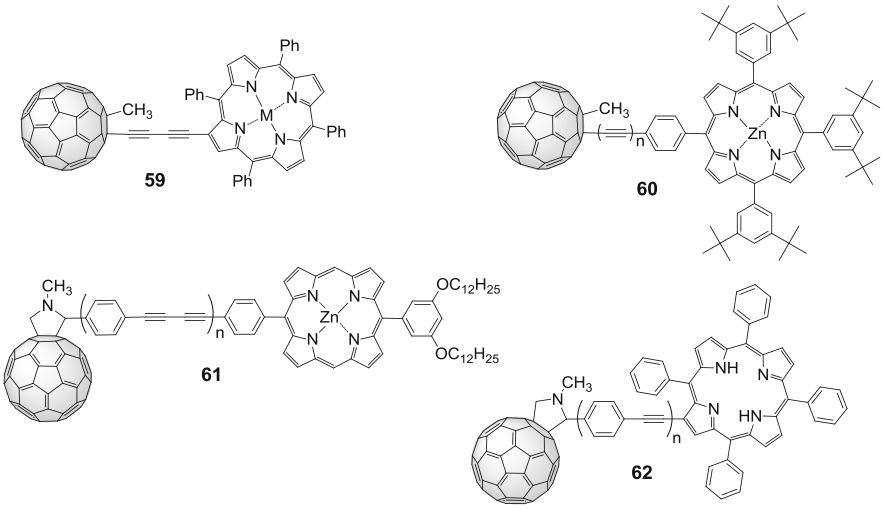

Fig. 32 Chemical structures of some ZnP/C_{60} conjugates

with increasing distance between the donor and acceptor moieties is observed, which implies a through-bond mechanism where the bridge plays an important role. A damping factor of 0.11 ± 0.05 Å^{-1} has been determined for these compounds [247]. This value is lower than the β value reported for similar systems bearing exTTF as donor moiety (exTTF-oPPE-C_{60}), for which an attenuation factor of 0.21 Å^{-1} was determined. This difference has been accounted for by a much more uniform distribution of the local electron affinity in ZnP–oPPE–C_{60} **62** due to higher electron density of ZnP in comparison to exTTF. These results underline the dependence of the β value and hence the wire-like behavior on the whole DBA system and not only on the linker.

An extraordinarily small attenuation factor of 0.01 ± 0.005 Å^{-1} was determined for compounds in which the donor exTTF and the acceptor C_{60} are connected through a *p*-phenylenevinylene oligomer **63** (exTTF–oPPV–C_{60}) [248, 249]. This low β value has been explained attending to the *para*-conjugation of the bridge with the donor exTTF and the homogeneous distribution of the local electron affinity throughout the whole bridge. A remarkable value of ~5.5 cm^{-1} for the coupling constant (V) was determined for these systems, unusually strong over a distance of 40 Å from the electron donor to the electron acceptor. Analogous systems in which the donor moiety has been substituted by a porphyrin **66** (ZnP–oPPV–C_{60}) give rise to a slightly higher β value (0.03 ± 0.005 Å^{-1}) due probably to a loss of conjugation between the donor ZnP and the linker [250] (Fig. 33).

The systematic study of the wire-like behavior in systems in which ZnP/C_{60} conjugates are connected through a *para*-cyclophane–oPPV (pCp–oPPV) bridge has shown a β value of 0.039 ± 0.001 Å^{-1}. The inhomogeneous and weaker

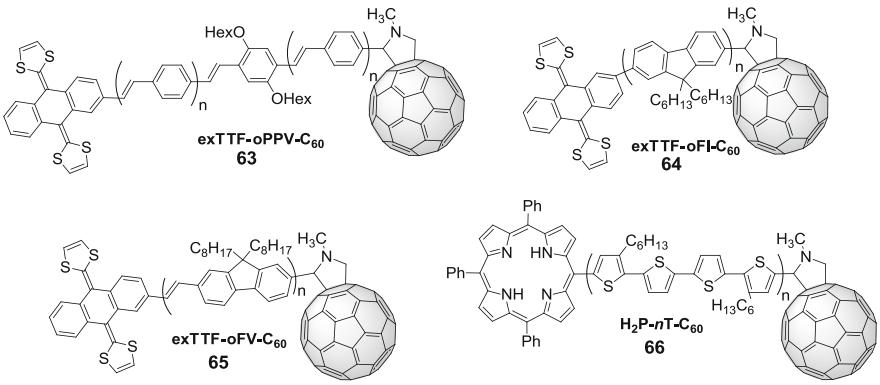

Fig. 33 Oligophenylenevinylene, oligofluorene, oligofluorenevinylene, and polythiophene donor/acceptor conjugates

π-conjugation of pCp–oPPV related to oPPV accounts for the approximately four times greater damping factor [251].

The comparison of the charge transfer characteristics of oligofluorenes (oFl) **64** vs oligofluorenevinylenes (oFV) **65** shows that it is possible to tune the electronic properties by slight structural alterations of the compounds. Specifically, β values of 0.075 $Å^{-1}$ are obtained for the oFV wires, lower than the value determined for oFl (0.09 $Å^{-1}$) [252]. The vinylene groups improve the π-conjugation of the wire in such a way that charge injection into the bridge is favored, facilitating CS and CR processes [253].

When oligothiophenes (nT) are employed as bridges, distances up to 55.7 Å have been reached between D and A. For these H_2P–nT–C_{60} systems, a dependency of the β value on solvent polarity was observed (0.11 $Å^{-1}$ in *o*-dichlorobenzene and 0.03 $Å^{-1}$ in benzonitrile) [254, 255]. Due to the electron-donating ability of the polythiophene oligomers, these bridges participate more actively in the CS/CR processes, which take place almost via the electron-hopping mechanism.

Recently, supramolecular ZnP/C_{60} hybrids connected by a Hamilton receptor and employing different spacers as oPPE, oPPV, *p*-ethynylene, or fluorene have been systematically studied [256]. These studies demonstrate that the electronic communication between the donor and acceptor moieties is governed by the charge transfer properties of the conjugated spacers. Thus, spacers with low β values facilitate the charge transfer along the supramolecular bridge. The study of the dependence of the rate constants of CS and CR on the D–A distances allowed the calculation of the attenuation factor for the first time in a hydrogen-bonding-mediated electron transfer, rendering a value of 0.11 $Å^{-1}$, which is similar to that obtained for other covalent systems (Fig. 34).

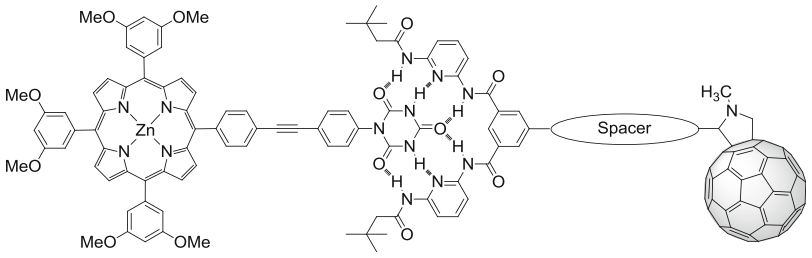

67

Fig. 34 Supramolecular ZnP/C_{60} molecular wire

7 The Future: Non-IPR Fullerenes

As stated above, C_{60} is by far the most abundant and common of all fullerenes. The question is why, among the many possible cages that can be formed with carbon atoms, the one containing 60 atoms is favored? Furthermore, since all fullerenes Cn are constituted by hexagons ($n \geq 20$ with the exception of $n = 22$) and pentagons (12 for all fullerene cages, which are responsible for the curved geometry), why among the 1,812 possible isomers for 60 carbon atoms was only the icosahedral symmetry I_h-C_{60} molecule (soccer-ball shape) formed?

These intriguing questions were answered by Kroto, who proposed that the local strain increases with the number of bonds shared by two pentagons (pentalene units), thus affording less-stable molecules. This rule was coined as the "isolated pentagon rule" (IPR), stating that all pentagons must be surrounded by hexagons, thus forming the corannulene moiety [16]. The resonance destabilization that results from the adjacent pentagons (8π electrons which do not satisfy the Hückel rule) and reduction of the π-orbital overlapping because of cage curvature explains the lower stability of non-IPR fullerenes [257]. A head-to-tail exclusion rule has also been proposed to explain the higher stability of fullerenes obeying the IPR rule [258].

For a precise number of carbon atoms forming a cage, the number of non-IPR fullerene isomers is very much larger than the IPR ones. Furthermore, in addition to doubly fused pentagons found in non-IPR fullerenes, triple directly fused pentagons and more recently triple sequentially fused pentagons have been reported [259]. Therefore there is great interest in the search for the huge number of expected non-IPR fullerenes whose chemical reactivity and properties should be different from those known for IPR fullerenes [260].

In order to achieve non-IPR fullerenes, two different strategies have been developed to increase their stability, namely through endohedral and exohedral derivatization [261]. In both approaches the key issue to stabilize non-IPR fullerenes focuses on how to release or decrease the strains of fused pentagons.

The first endohedral strategy involves encaging a metal cluster inside the fullerene cage. The bending strain on fused pentagons is significantly decreased

because of the strong interactions between the fused pentagons and the metal cluster.

Endohedral fullerenes have been known from the earliest times of fullerenes (see above). Although theoretical studies predicted in the early 1990s that elusive non-IPR fullerenes could be stabilized by the presence of clusters encapsulated in the fullerene cage, the first non-IPR fullerenes, namely $Sc_2@C_{66}$ [262] and $Sc_3N@C_{68}$ [263], were obtained in 2000. It is important to note that carbon cages in endohedral fullerenes are different from those observed in empty fullerenes. Therefore, favorable electronic interactions between the encapsulated species with the carbon cage are required for the stabilization of the resulting endohedral fullerene.

This method brings about the productions of other different non-IPR metallofullerenes, such as trimetallic nitride fullerenes (i.e., $Tb_3N@C_{84}$ [264], $Sc_3N@C_{70}$ [265], and $Y_3N@C_{78}$ [266] etc.), metal carbide endofullerene $Sc_2C_2@C_{68}$ [267], and metal cyanide endofullerene $Sc_3NC@C_{78}$ [268].

A simple and qualitative rule to predict the stability of a given endohedral is based on the calculated HOMO–LUMO gap for the resulting "ionic" endofullerene. This energy gap can be roughly calculated from the (LUMO-3)–(LUMO-4) gap determined for the neutral cage, thus predicting the most stable IPR and non-IPR endofullerenes [269].

Remarkably, non-IPR endohedral metallofullerenes (fullerenes containing one or more metal atoms in the inner cavity) show a strong coordination of the metal atoms to the fused pentagons, similar to that observed for a variety of organometallic species in which the concave face of the pentalene unit is coordinated to the metal atom [270]. In contrast, IPR endofullerenes show a motion for the encapsulated metals or clusters in the inner cavity. In some cases involving endofullerenes endowed with only one metal atom, the metal generally coordinates with the cage and motion is difficult.

On the other hand, the second strategy based on exohedral derivatization has afforded a variety of non-IPR derivatives based on the remarkable reactivity of the fused pentagons, thus changing the carbon bond hybridization and releasing the bending strains. The first small fullerene $^{\#271}C_{50}$ (the Fowler–Manolopoulos nomenclature to differentiate isomers is specified by symmetry and/or by spiral algorithm) was trapped and stabilized by chlorine atoms as $^{\#271}C_{50}Cl_{10}$ in 2004 [271]. Since then the fullerene cage has been exohedrically functionalized by introducing hydrogen or chloride atoms on the cage surface, to produce a variety of non-IPR fullerene derivatives, such as $C_{64}H_4$ [272], $C_{71}H_2$ [273], $C_{78}Cl_8$ [274], etc.

This stabilization of the resulting non-IPR fullerene derivatives has been accounted for by the "strain-relief principle" resulting from the rehybridization from sp^2 to sp^3 carbon atoms, as well as by the "local aromaticity principle," which involves maintaining the local aromaticity of the un-derivatized sp^2 carbon skeleton that remains after the derivatization process. Based on both principles, it has been possible to predict the stability of a variety of exohedrically functionalized non-IPR fullerenes.

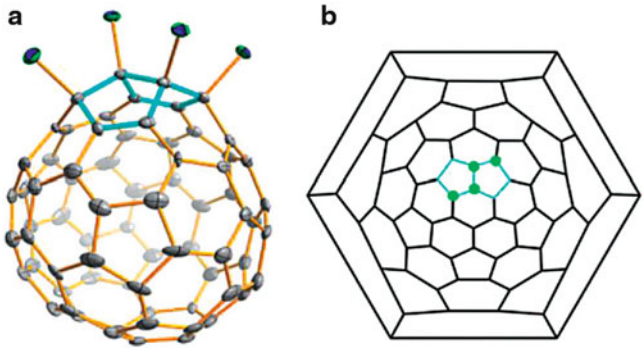

Fig. 35 X-ray structure of non-IPR $^{\#11188}C_{72}Cl_4$. (**a**) Fused pentagons are shown in *blue*. (**b**) Schlegel diagram showing the position of the four chlorine atoms. (Reprinted with permission from [279].)

Particular attention has been devoted to the structure of fullerene C_{72}, a so-called "missing fullerene" because empty C_{72}, IPR or non-IPR isomer, had never been isolated. However, along with further studies, recently several C_{72}-based species have been successfully prepared and characterized, namely $La_2@D_2(10611)$-C_{72} [275], $Ce_2@D_2(10611)$-C_{72} [276], $La@C_2(10612)$-C_{72} [277], and $Sc_2S@Cs(10528)$-C_{72} [278].

Experimental results have recently reported, for the first time, the higher stability of a non-IPR fullerene compared to its related IPR isomer for $C_{72}Cl_4$ [279, 280] (Fig. 35). These new results violate the "universal" IPR rule for fullerenes, but confirm the valuable "strain-release" and "local aromaticity" principles that have been so useful to predict the stability of a wide variety of fullerene derivatives. The IPR rule is therefore valid for pristine fullerenes, whereas for fullerene derivatives additional factors emerge that could eventually force a non-IPR cage to be the most stable one. These new results pave the way to the advent of a huge family of, so far, unknown non-IPR fullerenes whose number would be almost infinite. These thermodynamically less stable carbon cages should exhibit significant differences compared to those IPR obeying fullerenes, thus enhancing the properties and applications of these molecular allotropes of carbon. The scientific community should be ready for the advent of the unprecedented non-IPR fullerenes, the fullerenes for the near future!

8 Summary, Conclusions, Outlook

In the above sections we have presented some of the important achievements in the past few years with buckyballs from the viewpoint of a synthetic chemist and with an eye on the most remarkable properties of these molecules of interest for practical purposes, namely in organic electronics.

Fullerenes form a broad family of carbon nanostructures which, in principle, must obey the IPR rule as a criteria of stability. The so-called hollow fullerenes undergo a very rich covalent chemistry affording a wide variety of fullerene derivatives. In this review we have mainly focussed on those reactions carried out involving metals as catalysts, which have significantly enhanced the scope of derivatives prepared so far. Furthermore, in our group we reported the detailed retro-cycloaddition reaction of well-known fullerenopyrrolidines in a quantitative manner, thus providing a new protection–deprotection protocol in fullerene chemistry. This interesting reaction was later extended to other fullerene cycloadducts.

An important topic is combining the intriguing properties of fullerenes with those of highly versatile polymers, affording the new interdisciplinary field of "fullerene polymers." This field has been reviewed with the most outstanding and recent advances and applications according to the rational structural classification given in the text.

The convex surface of fullerenes is an ideal scenario to interact with the concave surface of different organic molecules. Therefore the supramolecular chemistry of fullerenes has been presented with special emphasis on H-bonding interactions and π,π concave–convex interactions in which our group has been mainly engaged. This singular approach has been complemented with the most significant examples in the search for fullerene receptors from other authors.

Just a few years have been enough to show that the carbon family is much larger than initially thought and many other forms of carbon, sometimes encapsulating atoms, molecules, or clusters in their inner cavity (endohedral fullerenes), have been produced. Although the number of endohedral fullerenes is becoming larger and larger and new chemical species are placed at the inner cavity of fullerenes, the most frequent and studied endofullerenes have been presented according to their properties and chemical reactivity, thus complementing the related hollow fullerenes.

The applications of fullerenes is an open question which has been mainly focussed on the use of fullerenes for organic electronics, namely with their use in organic photovoltaics which, no doubt, represents the most realistic application of fullerenes, as well as their use in the study of molecular wires. Both topics give an idea of the interest of these carbon allotropes in the emerging fields of nanoscience and nanotechnology.

Finally, we have stressed the future of fullerenes on those which are nowadays considered an almost scientific curiosity, the non-IPR fullerenes. Since they are thermodynamically less stable than the corresponding fullerenes obeying the IPR rule, their syntheses as endo- or exohedrically functionalized species is currently a synthetic challenge and some of the most outstanding examples have been presented. Since the potential number is huge compared with those known so far, the history and development of fullerenes might just be in its infancy. The future will tell us how these and other fullerene species still to come will impact new technologies based on these new carbon nanoforms.

References

1. Kroto HW, Heath JR, O'Brien SC et al (1985) C_{60}: buckminsterfullerene. Nature 318:162–163
2. Cami J, Bernard-Salas J, Peeters E et al (2010) Detection of C_{60} and C_{70} in a young planetary nebula. Science 329:1180–1182
3. Iijima S (1991) Helical microtubules of graphitic carbon. Nature 354:56–58
4. Iijima S, Ichihashi T (1993) Single-shell carbon nanotubes of 1-nm diameter. Nature 363:603–605
5. Bethune DS, Kiang CH, de Vries MS et al (1993) Cobalt-catalyzed growth of carbon nanotubes with single-atomic-layer walls. Nature 363:605–607
6. Novoselov KS, Geim AK, Morozov SV et al (2004) Electric field effect in atomically thin carbon films. Science 306:666–669
7. Delgado JL, Herranz MA, Martín N (2008) The nanoforms of carbon. J Mater Chem 18:1417–1426
8. Akasaka T, Nagase S (2002) Endofullerenes: a new family of carbon cluster. Kluwer, Dordrecht
9. Kroto HW (1997) Symmetry, space, stars, and C_{60}. Angew Chem Int Ed 36:1578–1593
10. Smalley RE (1997) Discovering the fullerrenes. Angew Chem Int Ed 36:1594–1601
11. Curl RF (1997) Dawn of the fullerenes: conjecture and experiment. Angew Chem Int Ed 36:1566–1576
12. Martín N (2006) New challenges in fullerene chemistry. Chem Commun 2093–2104
13. Krätschmer W, Lamb LD, Fostiropoulos K et al (1990) Solid C_{60}: a new form of carbon. Nature 347:354–358
14. Jones DEH (1966) Hollow molecules. New Sci 32:245
15. Chuvilin A, Kaiser U, Bichoutskaia E et al (2010) Direct transformation of graphene to fullerene. Nat Chem 2:450–453
16. Kroto HW (1987) The stability of the fullerenes C_n, with $n = 24, 28, 32, 36, 50, 60$ and 70. Nature 329:529–531
17. Haddon RC (1992) Electronic structure, conductivity, and superconductivity of alkali metal doped C_{60}. Acc Chem Res 25:127–133
18. Hirsch A, Chen Z, Jiao H (2000) Spherical aromaticity in I_h symmetrical fullerenes: the $2(N + 1)^2$ rule. Angew Chem Int Ed 39:3915–3917
19. Guldi DM, Martín N (eds) (2002) Fullerenes: from synthesis to optoelectronic properties. Kluwer Academic, Dordrecht
20. Hirsch A, Brettreich M (2005) Fullerenes, chemistry and reactions. Wiley-VCH, Weinheim
21. Langa F, Nierengarten JF (eds) (2012) Fullerenes: principles and applications. Royal Society of Chemistry, Cambridge
22. Haddon RC, Brus LE, Raghavachari K (1986) Electronic structure and bonding in icosahedral carbon cluster (C_{60}). Chem Phys Lett 125:459–464
23. Xie Q, Perez-Cordero E, Echegoyen L (1992) Electrochemical detection of C_{60} and C_{70}: enhanced stability of fullerides in solution. J Am Chem Soc 114:3978–3980
24. Martin N, Altable M, Filippone S et al (2006) Thermal [2+2] intramolecular cycloadditions of fuller-1,6-enynes. Angew Chem Int Ed 45:1439–1442
25. Altable M, Filippone S, Martin-Domenech A et al (2006) Intramolecular ene reaction of 1,6-fullerenynes: a new synthesis of allenes. Org Lett 8:5959–5962
26. Li H, Risko C, Seo JH et al (2011) Fullerene–carbene Lewis acid–base adducts. J Am Chem Soc 133:12410–12413
27. Cozzi F, Powell WH, Thilgen C (2005) Numbering of fullerenes. Pure Appl Chem 77:843–923
28. Komatsu K, Murata Y, Takimoto N et al (1994) Synthesis and properties of the first acetylene derivatives of C_{60}. J Org Chem 59:6101–6102

29. Nagashima H, Terasaki H, Kimura E et al (1994) Silylmethylations of C_{60} with Grignard reagents: selective synthesis of $HC_{60}CH_2SiMe_2Y$ and $C_{60}(CH_2SiMe_2Y)_2$ with selection of solvents. J Org Chem 59:1246–1248
30. Hirsch A, Soi A, Karfunhel HR (1992) Titration of C_{60}: a method for the synthesis of organofullerenes. Angew Chem Int Ed 31:766–768
31. Sawamura M, Iikura H, Nakamura E (1996) The first pentahaptofullerene metal complexes. J Am Chem Soc 118:12850–12851
32. Matsuo Y, Nakamura E (2008) Selective multiaddition of organocopper reagents to fullerenes. Chem Rev 108:3016–3028
33. Martin N, Altable M, Filippone S et al. (2004) Highly efficient Pauson–Khand reaction with C_{60}: regioselective synthesis of unprecedented *cis*-1 biscycloadducts. Chem Commun 1338–1339
34. Martín N, Altable M, Filippone S et al (2005) Regioselective intramolecular Pauson–Khand reactions of C_{60}: an electrochemical study and theoretical underpinning. Chemistry 11:2716–2729
35. Nambo M, Noyori R, Itami K (2007) Rh-catalyzed arylation and alkenylation of C_{60} using organoboron compounds. J Am Chem Soc 129:8080–8081
36. Nambo M, Segawa Y, Wakamiya A et al (2011) Selective introduction of organic groups to C_{60} and C_{70} using organoboron compounds and rhodium catalyst: a new synthetic approach to organo(hydro)fullerenes. Chem Asian J 6:590–598
37. Lu S, Jin T, Bao M et al (2011) Cobalt-catalyzed hydroalkylation of [60]fullerene with active alkyl bromides: selective synthesis of monoalkylated fullerenes. J Am Chem Soc 133:12842–12848
38. Xiao Z, Matsuo Y, Nakamura E (2010) Copper-catalyzed formal [4+2] annulation between alkyne and fullerene bromide. J Am Chem Soc 132:12234–12236
39. Zhu B, Wang G-W (2009) Palladium-catalyzed heteroannulation of [60]fullerene with anilides via C–H bond activation. Org Lett 11:4334–4337
40. Thilgen C, Gosse I, Diederich F (2003) Chirality in fullerene chemistry. Top Stereochem 23:1–124
41. Thilgen C, Diederich F (2006) Structural aspects of fullerene chemistry: a journey through fullerene chirality. Chem Rev 106:5049–5135
42. Nishimura T (2004) Macromolecular helicity induction on a poly(phenylacetylene) with C_2-symmetric chiral [60]fullerene-bisadducts. J Am Chem Soc 126:11711–11717
43. Friedman SH, Ganapathi PS, Rubin Y et al (1998) Optimizing the binding of fullerene inhibitors of the HIV-1 protease through predicted increases in hydrophobic desolvation. J Med Chem 41:2424–2429
44. Hizume Y, Tashiro K, Charvet R et al (2010) Chiroselective assembly of a chiral porphyrin–-fullerene dyad: photoconductive nanofiber with a top-class ambipolar charge-carrier mobility. J Am Chem Soc 132:6628–6629
45. Filippone S, Maroto EE, Martín-Domenech A et al (2009) An efficient approach to chiral fullerene derivatives by catalytic enantioselective 1,3-dipolar cycloadditions. Nat Chem 1:578–582
46. Maroto EE, Filippone S, Martin-Domenech A et al (2012) Switching the stereoselectivity: (fullero)pyrrolidines “a la carte”. J Am Chem Soc 134:12936–12938
47. Maroto EE, de Cózar A, Filippone S et al (2011) Hierarchical selectivity in fullerenes: site-, regio-, diastereo-, and enantiocontrol of the 1,3-dipolar cycloaddition to C70. Angew Chem Int Ed 50:6060–6064
48. Sawai K, Takano Y, Izquierdo M et al (2011) Enantioselective synthesis of endohedral metallofullerenes. J Am Chem Soc 133:17746–17752
49. Bosi S, Da Ros T, Spalluto G et al (2003) Fullerene derivatives: an attractive tool for biological applications. Eur J Med Chem 38:913–923
50. Prato M, Martín N (eds) (2002) Special issue: Functionalised fullerenes. J Mater Chem 12:1931–2159

51. Manoharan M, de Proft F, Geerlings P (2000) Aromaticity interplay between quinodimethanes and C60 in Diels–Alder reactions: insights from a theoretical study. J Org Chem 65:6132–6137
52. Kräutler B, Maynollo J (1995) A highly symmetric sixfold cycloaddition product of fullerene C_{60}. Angew Chem Int Ed Engl 34:87–88
53. Herranz MA, Martín N, Ramey J et al (2002) Thermally reversible C_{60}-based donor–acceptor ensembles. Chem Commun 2002:2968–2969
54. Bingel C (1993) Cyclopropanierung von fullerenen. Chem Ber 126:1957–1959
55. Kessinger R, Crassous J, Herrmann A et al (1998) Preparation of enantiomerically pure C_{76} with a general electrochemical method for the removal of di(alkoxycarbonyl)methano bridges from methanofullerenes: the retro-Bingel reaction. Angew Chem Int Ed 37:1919–1922
56. Kessinger R, Fender NS, Echegoyen LE et al (2000) Selective electrolytic removal of bis (alkoxycarbonyl)methano addends from C_{60} bis-adducts and electrochemical stability of C_{70} derivatives. Chemistry 6:2184–2192
57. Moonen NNP, Thilgen C, Echegoyen L et al (2000) The chemical retro-Bingel reaction: selective removal of bis(alkoxycarbonyl)methano addends from C_{60} and C_{70} with amalgamated magnesium. Chem Commun 5:335–336
58. Prato M, Maggini M (1998) Fulleropyrrolidines: a family of full-fledged fullerene derivatives. Acc Chem Res 31:519–526
59. Martín N, Altable M, Filippone S et al (2006) Retro-cycloaddition reaction of pyrrolidinofullerenes. Angew Chem Int Ed 45:110–114
60. Brunetti FG, Herrero MA, Muñoz JM et al (2007) Reversible microwave-assisted cycloaddition of aziridines to carbon nanotubes. J Am Chem Soc 129:14580–14581
61. Guryanov I, Montellano Lopez A, Carraro M et al (2009) Metal-free, retro-cycloaddition of fulleropyrrolidines in ionic liquids under microwave irradiation. Chem Commun 3940–3942
62. Filippone S, Izquierdo Barroso M, Martín-Domenech A et al (2008) On the mechanism of the thermal retrocycloaddition of pyrrolidinofullerenes (retro-Prato reaction). Chemistry 14:5198–5206
63. Lukoyanova O, Cardona CM, Altable M et al (2006) Selective electrochemical retro-cycloaddition reaction of pyrrolidinofullerenes. Angew Chem Int Ed 45:7430–7433
64. Martín N, Altable M, Filippone S et al (2007) Highly efficient retro-cycloaddition reaction of isoxazolino[4,5:1,2][60]- and -[70]fullerenes. J Org Chem 72:3840–3846
65. Delgado JL, Oswald F, Cardinali F et al (2008) On the thermal stability of [60]fullerene cycloadducts: retro-cycloaddition reaction of 2-pyrazolino[4,5:1,2][60]-fullerenes. J Org Chem 73:3184–3188
66. Olah GA, Bucsi I, Lambert C et al (1991) Polyarenefullerenes, $C_{60}(H\text{-}Ar)_n$, obtained by acid-catalyzed fullerenation of aromatics. J Am Chem Soc 113:9387–9388
67. Giacalone F, Martín N (2006) Fullerene polymers: synthesis and properties. Chem Rev 106:5136–5190
68. Giacalone F, Martín N (eds) (2009) Fullerene polymers: synthesis, properties and applications. Wiley VCH, Weinheim
69. Giacalone F, Martín N (2010) New concepts and applications in the macromolecular chemistry of fullerenes. Adv Mater 22:4220–4248
70. Special issue on polymeric fullerenes (1997) Appl Phys A: Mater Sci Process 64:223–330
71. Sundqvist B (1999) Fullerenes under high pressures. Adv Phys 48:1
72. Rao AM, Zhou P, Wang K-A et al (1993) Photo-induced polymerization of solid C_{60} films. Science 259:955–957
73. Iwasa Y, Arima T, Fleming RM et al (1994) New phases of C_{60} synthesized at high-pressure. Science 264:1570–1572
74. Takahashi N, Dock H, Matsuzawa N et al (1993) Plasma-polymerized C_{60}/C_{70} mixture films: electric conductivity and structure. J Appl Phys 74:5790–5798

75. Nuñez-Regueiro M, Marques L, Hodeau JL et al (1995) Polymerized fullerite structures. Phys Rev Lett 74:278–281
76. Rao AM, Eklund PC, Venkateswaran UD et al (1997) Properties of C_{60} polymerized under high pressure and temperature. Appl Phys A: Mater Sci Process 64:231–2239
77. Fedurco M, Costa DA, Balch AL et al (1995) Electrochemical synthesis of a redox-active polymer based on buckminsterfullerene epoxide. Angew Chem Int Ed Engl 34:194–196
78. Winkler K, Costa DA, Balch AL et al (1995) A study of fullerene epoxide electroreduction and electropolymerization processes. J Phys Chem 99:17431–17436
79. Liu B, Bunker CE, Sun T-P (1996) Preparation and characterization of soluble pendant [60] fullerene-polystyrene polymers. Chem Commun 1241–1242
80. Stalmach U, de Boer B, Videlot C et al (2000) Semiconducting diblock copolymers synthesized by means of controlled radical polymerization techniques. J Am Chem Soc 122:5464–5472
81. Zheng JW, Goh SH, Lee SY (2000) Miscibility of C_{60}-containing poly(methyl methacrylate)/poly(vinylidene fluoride) blends. J Appl Polym Sci 75:1393–1396
82. Wang C, Tao Z, Yang W et al (2001) Synthesis and photoconductivity study of C_{60}-containing styrene/acrylamide copolymers. Macromol Rapid Commun 22:98–103
83. Gutiérrez-Nava M, Masson P, Nierengarten J-F (2003) Synthesis of copolymers alternating oligophenylenevinylene subunits and fullerene moieties. Tetrahedron Lett 44:4487–4490
84. Vitalini D, Mineo P, Iudicelli V et al (2000) Preparation of functionalized copolymers by thermal processes: porphyrination and fullerenation of a commercial polycarbonate. Macromolecules 33:7300–7309
85. Kraus A, Müllen K (1999) [60]Fullerene-containing poly(dimethylsiloxane)s: easy access to soluble polymers with high fullerene content. Macromolecules 32:4214–4219
86. Ungurenasu C, Pienteala M (2007) Syntheses and characterization of water-soluble C_{60}–curdlan sulfates for biological applications. J Polym Sci Part A: Polym Chem 45:3124–3128
87. Cravino A, Sariciftci NS (2002) Double-cable polymers for fullerene based organic optoelectronic applications. J Mater Chem 12:1931–1943
88. Cravino A, Sariciftci NS (2003) Organic electronics: molecules as bipolar conductors. Nat Mater 2:360–361
89. Kawase T (2012) Receptors for pristine fullerenes based on concave-convex π-π interactions. In: Martín N, Nierengarten J-F (eds) Supramolecular chemistry of fullerenes and carbon nanotubes. Wiley-VCH, Weinheim, pp 55–78 (Chap. 3)
90. Martín N, Nierengarten J-F (2012) Supramolecular chemistry of fullerenes and carbon nanotubes. Wiley-VCH, Weinheim
91. Sterescu DM, Stamatialis DF, Mendes E, Wibbenhorst M, Wessling M (2006) Fullerene-modified poly(2,6-dimethyl-1,4-phenylene oxide) gas separation membranes: why binding is better than dispersing. Macromolecules 39:9234–9242
92. Vinogradova LV, Polotskaya GA, Shevtsova AA et al (2009) Gas-separating properties of membranes based on star-shaped fullerene (C_{60})-containing polystyrenes. Polym Sci Ser A 51:209–215
93. Wang H, DeSousa R, Gasa J et al (2007) Fabrication of new fullerene composite materials and their application in proton exchange membrane fuel cells. J Membr Sci 289:277–283
94. Chen X, Gholamkhass B, Han X et al (2007) Polythiophene-*graft*-styrene and polythiophene-*graft*-(styrene-*graft*-C_{60}) copolymers. Macromol Rapid Commun 28:1792–1797
95. Nanjo M, Cyr PW, Liu K et al (2008) Donor–acceptor C_{60}-containing polyferrocenylsilanes: synthesis, characterization, and applications in photodiode devices. Adv Funct Mater 18:470–477
96. Ling Q-D, Lim S-L, Song Y et al (2007) Nonvolatile polymer memory device based on bistable electrical switching in a thin film of poly(*N*-vinylcarbazole) with covalently bonded C_{60}. Langmuir 23:312–319

97. Tutt LW, Kost A (1992) Optical limiting performance of C_{60} and C_{70} solutions. Nature 356:225–226
98. Cha M, Sariciftci NS, Heeger AJ et al (1995) Enhanced nonlinear absorption and optical limiting in semiconducting polymer/methanofullerene charge transfer films. Appl Phys Lett 67:3850–3852
99. Maggini M, Scorrano G, Prato M et al (1995) C_{60} derivatives embedded in sol–gel silica films. Adv Mater 7:404–406
100. Bunker CE, Lawson GE, Sun YP (1995) Fullerene-styrene random copolymers. Novel optical properties. Macromolecules 28:3744–3746
101. Kojima Y, Matsuoka T, Takahashi H et al (1995) Optical limiting property of polystyrene-bound C_{60}. Macromolecules 28:8868–8869
102. Lu Z, Goh SH, Lee SY et al (1999) Synthesis, characterization and nonlinear optical properties of copolymers of benzylaminofullerene with methyl methacrylate or ethyl methacrylate. Polymer 40:2863–2867
103. Sun YP, Riggs JE (1997) Non-linear absorptions in pendant [60]fullerene–polystyrene polymers. J Chem Soc Faraday Trans 93:1965–1969
104. Tang BZ, Xu HY, Lam JWY et al (2000) C_{60}-containing poly(1-phenyl-1-alkynes): synthesis, light emission, and optical limiting. Chem Mater 12:1446–1449
105. Li FY, Li YL, Guo ZX et al (2000) Synthesis and optical limiting properties of polycarbonates containing fullerene derivative. J Phys Chem Solids 61:1101–1103
106. Celli A, Marchese P, Vannini M et al (2011) Synthesis of novel fullerene-functionalized polysulfones for optical limiting applications. React Funct Polym 71:641–647
107. Mroz P, Tegos GP, Gali H et al (2007) Photodynamic therapy with fullerenes. Photochem Photobiol Sci 6:1139–1149
108. Liu Y, Wang H, Liang P et al (2004) Water-soluble supramolecular fullerene assembly mediated by metallobridged β-cyclodextrins. Angew Chem Int Ed 43:2690–2694
109. Samal S, Choi B-J, Geckeler KE (2001) DNA-cleavage by fullerene-based synzymes. Macromol Biosci 1:329–331
110. Liu J, Ohta S, Sonoda A et al (2007) Preparation of PEG-conjugated fullerene containing Gd^{3+} ions for photodynamic therapy. J Control Release 117:104–110
111. Stoilova O, Jérôme C, Detrembleur C et al (2007) C_{60}-containing nanostructured polymeric materials with potential biomedical applications. Polymer 48:1835–1843
112. Drees M, Hoppe H, Winder C et al (2005) Stabilization of the nanomorphology of polymer–fullerene "bulk heterojunction" blends using a novel polymerizable fullerene derivative. J Mater Chem 15:5158–5163
113. Sivula K, Ball ZT, Watanabe N et al (2006) Amphiphilic diblock copolymer compatibilizers and their effect on the morphology and performance of polythiophene:fullerene solar cells. Adv Mater 18:206–210
114. Yang C, Lee JK, Heeger AJ et al (2009) Well-defined donor–acceptor rod–coil diblock copolymers based on P3HT containing C_{60}: the morphology and role as a surfactant in bulk-heterojunction solar cells. J Mater Chem 19:5416–5423
115. Hsieh C-H, Cheng Y-J, Li P-J et al (2010) Highly efficient and stable inverted polymer solar cells integrated with a cross-linked fullerene material as an interlayer. J Am Chem Soc 132:4887–4893
116. Cheng Y-J, Hsieh C-H, He Y et al (2010) Combination of indene-C_{60} bis-adduct and cross-linked fullerene interlayer leading to highly efficient inverted polymer solar cells. J Am Chem Soc 132:17381–17383
117. Jeffery GA (1997) An introduction to hydrogen bonding. Oxford University Press, Oxford
118. Collins AF, Critchley C (2005) Artificial photosynthesis: from basic biology to industrial applications. Wiley, Weinheim
119. Delgado JL, Bouit PA, Filippone S et al (2010) Organic photovoltaics: a chemical approach. Chem Commun 46:4853–4865

120. Pinzón JR, Villalta-Cerdas A, Echegoyen L (2012) Fullerenes, carbon nanotubes, and graphene for molecular electronics. Top Curr Chem 312:127–174
121. Diederich F, Echegoyen L, Gómez-López M et al (1999) The self-assembly of fullerene-containing [2]pseudorotaxanes: formation of a supramolecular C_{60} dimer. J Chem Soc Perkin Trans 2:1577–1586
122. Rispens MT, Sánchez L, Knol J et al (2001) Supramolecular organization of fullerenes by quadruple hydrogen bonding. Chem Commun 161–162
123. González JJ, González S, Priego E et al (2001) A new approach to supramolecular C_{60}-dimers based in quadruple hydrogen bonding. Chem Commun 163–164
124. Da Ros T, Guldi DM, Morales AF et al (2003) Hydrogen bond-assembled fullerene molecular shuttle. Org Lett 5:689–691
125. Mateo-Alonso A, Fioravanti G, Marcaccio M et al (2006) Reverse shuttling in a fullerene-stoppered rotaxane. Org Lett 8:5173–5176
126. Mateo-Alonso A, Brough P, Prato M (2007) Stabilization of fulleropyrrolidine N-oxides through intrarotaxane hydrogen bonding. Chem Commun 1412–1414
127. Mateo-Alonso A, Fioravanti G, Marcaccio M et al (2007) An electrochemically driven molecular shuttle controlled and monitored by C_{60}. Chem Commun 1945–1947
128. Scarel F, Valenti G, Gaikwad S et al (2012) A molecular shuttle driven by fullerene radical-anion recognition. Chemistry 44:14063–14068
129. Guldi DM, Ramey J, Martínez-Díaz MV et al (2002) Reversible zinc phthalocyanine fullerene ensembles. Chem Commun 2774–2775
130. Sánchez L, Sierra M, Martín N et al (2006) Exceptionally strong electronic communication through hydrogen bonds in porphyrin–C_{60} pairs. Angew Chem Int Ed 45:4637–4641
131. Sessler JL, Jayawickramarajah J, Gouloumis A et al (2005) Synthesis and photophysics of a porphyrin-fullerene dyad assembled through Watson–Crick hydrogen bonding. Chem Commun 1892–1894
132. Torres T, Gouloumis A, Sánchez-García D et al (2007) Photophysical characterization of a cytidine-guanosine tethered phthalocyanine-fullerene dyad. Chem Commun 292–294
133. Wessendorf F, Gnichwitz J-F, Sarova GH et al (2007) Implementation of a Hamilton-receptor-based hydrogen-bonding motif toward a new electron donor-acceptor prototype: electron versus energy transfer. J Am Chem Soc 129:16057–16071
134. Maurer K, Grimm B, Wessendorf F et al (2010) Self-assembling depsipeptide dendrimers and dendritic fullerenes with new *cis*- and *trans*-symmetric Hamilton receptor functionalized Zn–porphyrins: synthesis, photophysical properties and cooperativity phenomena. Eur J Org Chem 5010–5029
135. Grimm B, Schornbaum J, Jasch H et al (2012) Step-by-step self-assembled hybrids that feature control over energy and charge transfer. Proc Natl Acad Sci U S A 109:15565–15571
136. Santos J, Grimm B, Illescas BM et al (2008) Cooperativity between π-π and H-bonding interactions – a supramolecular complex formed by C_{60} and exTTF. Chem Commun 5993–5995
137. Huang C-H, McClenaghan ND, Kuhn A et al (2005) Enhanced photovoltaic response in hydrogen-bonded all-organic devices. Org Lett 7:3409–3412
138. Chu C-C, Raffy G, Ray D et al (2010) Self-assembly of supramolecular fullerene ribbons via hydrogen-bonding interactions and their impact on fullerene electronic interactions and charge carrier mobility. J Am Chem Soc 132:12717–12723
139. Pérez EM, Martín N (2008) Curves ahead: molecular receptors for fullerenes based on concave-convex complementarity. Chem Soc Rev 37:1512–1519
140. Tashiro K, Aida T (2007) Metalloporphyrin hosts for supramolecular chemistry of fullerenes. Chem Soc Rev 36:189–197
141. Kawase T, Kurata H (2006) Ball-, bowl-, and belt-shaped conjugated systems and their complexing abilities: exploration of the concave-convex π−π interaction. Chem Rev 106:5250–5273

142. Mizyed S, Georghiou PE, Bancu M et al (2001) Embracing C_{60} with multiarmed geodesic partners. J Am Chem Soc 123:12770–12774
143. Sygula A, Fronczek FR, Sygula R et al (2007) A double concave hydrocarbon buckycatcher. J Am Chem Soc 129:3842–3843
144. Pérez EM, Martín N (2010) Molecular tweezers for fullerenes. Pure Appl Chem 82:523–533
145. Kawase T, Darabi HR, Oda M (1996) Cyclic [6]- and [8]paraphenylacetylenes. Angew Chem Int Ed 35:2664–2666
146. Kawase T, Tanaka K, Fujiwara N et al (2003) Complexation of a carbon nanoring with fullerenes. Angew Chem Int Ed 42:1624–1628
147. Kawase T, Tanaka K, Seirai Y et al (2003) Complexation of carbon nanorings with fullerenes: supramolecular dynamics and structural tuning for a fullerene sensor. Angew Chem Int Ed 42:5597–5600
148. Omachi H, Segawa Y, Itami K (2012) Synthesis of cycloparaphenylenes and related carbon nanorings: a step toward the controlled synthesis of carbon nanotubes. Acc Chem Res 45:1378–1389
149. Iwamoto T, Watanabe Y, Sadahiro T et al (2011) Size-selective encapsulation of C_{60} by [10] cycloparaphenylene: formation of the shortest fullerene-peapod. Angew Chem Int Ed 50:8342–8344
150. Xia J, Bacon JW, Jasti R (2012) Gram-scale synthesis and crystal structures of [8]- and [10] CPP, and the solid-state structure of C_{60}·[10]CPP. Chem Sci 3:3018–3021
151. Pérez EM, Sánchez L, Fernández G et al (2006) exTTF as a building block for fullerene receptors. Unexpected solvent-dependent positive homotropic cooperativity. J Am Chem Soc 128:7172–7173
152. Gayathri SS, Wielopolski M, Pérez EM et al (2009) Discrete supramolecular donor-acceptor complexes. Angew Chem Int Ed 48:815–819
153. Pérez EM, Capodilupo AL, Fernández G et al (2008) Weighting non-covalent forces in the molecular recognition of C_{60}. Relevance of concave-convex complementarity. Chem Commun 4567–4569
154. Pérez EM, Martín N (2012) Chiral recognition of carbon nanoforms. Org Biomol Chem 10:3577–3583
155. Pérez EM, Sierra M, Sánchez L et al (2007) Concave tetrathiafulvalene-type donors as supramolecular partners for fullerenes. Angew Chem Int Ed 46:1847–1851
156. Haino T, Yanase M, Fukazawa Y (1998) Fullerenes enclosed in bridged calix[5]arenes. Angew Chem Int Ed 37:997–998
157. Uno H, Furukawa M, Fujimoto A et al (2011) Porphyrin molecular tweezers for fullerenes. J Porphyr Phthalocyanins 15:951–963
158. Sun D, Tham FS, Reed CA et al (2000) Porphyrin-fullerene host-guest chemistry. J Am Chem Soc 122:10704–10705
159. Sun D, Tham FS, Reed CA et al (2002) Supramolecular fullerene-porphyrin chemistry. Fullerene complexation by metalated "jaws porphyrin" hosts. J Am Chem Soc 124:6604–6612
160. Hosseini A, Taylor S, Accorsi G et al (2006) Calix[4]arene-linked bisporphyrin hosts for fullerenes: binding strength, solvation effects, and porphyrin-fullerene charge transfer bands. J Am Chem Soc 128:15903–15913
161. Ayabe M, Ikeda A, Shinkai S et al (2002) A novel [60]fullerene receptor with a Pd(II)-switched bisporphyrin cleft. Chem Commun 1032–1033
162. Fernández G, Pérez EM, Sánchez L et al (2008) Self-organization of electroactive materials: a head-to-tail donor-acceptor supramolecular polymer. Angew Chem Int Ed 47:1094–1097
163. Fernández G, Pérez EM, Sánchez L et al (2008) An electroactive dynamically polydisperse supramolecular dendrimer. J Am Chem Soc 130:2410–2411
164. Santos J, Pérez EM, Illescas BM et al (2011) Linear and hyperbranched electron-acceptor supramolecular oligomers. Chem Asian J 6:1848–1853

165. Fernández G, Sánchez L, Pérez EM et al (2008) Large exTTF-based dendrimers. Self-assembly and peripheral cooperative multiencapsulation of C_{60}. J Am Chem Soc 130:10674–10683
166. Canevet D, Pérez EM, Martín N (2011) Wraparound hosts for fullerenes: tailored macrocycles and cages. Angew Chem Int Ed 50:9248–9259
167. Tashiro K, Aida T, Zheng J-Y et al (1999) A cyclic dimer of metalloporphyrin forms a highly stable inclusion complex with C_{60}. J Am Chem Soc 121:9477–9478
168. Yanagisawa M, Tashiro K, Yamasaki M et al (2007) Hosting fullerenes by dynamic bond formation with an iridium porphyrin cyclic dimer: a "chemical friction" for rotary guest motions. J Am Chem Soc 129:11912–11913
169. Gil-Ramírez G, Karlen SD, Shundo A et al (2010) A cyclic porphyrin trimer as a receptor for fullerenes. Org Lett 12:3544–3547
170. Song J, Aratani N, Shinokubo H et al (2010) A porphyrin nanobarrel that encapsulates C_{60}. J Am Chem Soc 132:16356–16357
171. Zheng J-Y, Tashiro K et al (2001) Cyclic dimers of metalloporphyrins as tunable hosts for fullerenes: a remarkable effect of rhodium(III). Angew Chem Int Ed 40:1857–1861
172. Isla H, Gallego M, Pérez EM et al (2010) A bis-exTTF macrocyclic receptor that associates C_{60} with micromolar affinity. J Am Chem Soc 132:1772–1773
173. Canevet D, Gallego M, Isla H et al (2011) Macrocyclic hosts for fullerenes: extreme changes in binding abilities with small structural variations. J Am Chem Soc 133:3184–3190
174. Akasaka T, Wudl F, Nagase S (2010) Chemistry of nanocarbons. Wiley-VCH, Chichester
175. Yamada M, Akasaka T, Nagase S (2010) Endohedral metal atoms in pristine and functionalized fullerene cages. Acc Chem Res 43:92–102
176. Lu X, Akasaka T, Nagase S (2012) Chemistry of endohedral metallofullerenes: the role of metals. Chem Commun 47:5942–5957
177. Rodríguez-Fortea A, Balch AL, Poblet JM (2011) Endohedral metallofullerenes: a unique host-guest association. Chem Soc Rev 40:3551–3563
178. Dunsch L, Yang S (2007) Metal nitride cluster fullerenes: their current state and future prospects. Small 3:1298–1320
179. Stevenson S, Mackey MA, Stuart MA et al (2008) A distorted tetrahedral metal oxide cluster inside an icosahedral carbon cage. Synthesis, isolation, and structural characterization of $Sc_4(mu_3\text{-}O)_2@I_h\text{-}C_{80}$. J Am Chem Soc 130:11844–11845
180. Chaur MN, Melin F, Ortiz AL et al (2009) Chemical, electrochemical, and structural properties of endohedral metallofullerenes. Angew Chem Int Ed 48:7514–7538
181. Saunders M, Jiménez-Vázquez HA, Cross RJ et al (1993) Stable compounds of helium and neon. $He@C_{60}$ and $Ne@C_{60}$. Science 259:1428–1430
182. Kurotobi K, Murata Y (2011) A single molecule of water encapsulated in fullerene C_{60}. Science 333:613–616
183. Campanera JM, Bo C, Olmstead MM et al (2002) Bonding within the endohedral fullerenes $Sc_3N@C_{78}$ and $Sc_3N@C_{80}$ as determined by density functional calculations and reexamination of the crystal structure of $\{Sc_3N@C_{78}\}\cdot Co(OEP)\}\cdot 1.5(C_6H_6)\cdot 0.3(CHCl_3)$. J Phys Chem A 106:12356–12364
184. Aoyagi S, Nishibori E, Sawa H et al (2010) A layered ionic crystal of polar $Li@C_{60}$ superatoms. Nat Chem 2:678–683
185. Aoyagi S, Sado Y, Nishibori E et al (2012) Rock-salt-type crystal of thermally contracted C_{60} with encapsulated lithium cation. Angew Chem Int Ed 51:3377–3381
186. Chai Y, Guo T, Jin C et al (1991) Fullerenes with metals inside. J Phys Chem 95:7564–7568
187. Nagase S, Kobayashi K (1994) The ionization energies and electron affinities of endohedral metallofullerenes MC_{82}(M = Sc, Y, La): density functional calculations. J Chem Soc Chem Commun 1837–1838
188. Tsuchiya T, Sato K, Kurihara H et al (2006) Spin-site exchange system constructed from endohedral metallofullerenes and organic donors. J Am Chem Soc 128:14418–14419

189. Sato S, Seki S, Honsho Y et al (2011) Semi-metallic single-component crystal of soluble La@C_{82} derivative with high electron mobility. J Am Chem Soc 133:2766–2771
190. Feng L, Tsuchiya T, Wakahara T et al (2006) Synthesis and characterization of a bisadduct of La@C_{82}. J Am Chem Soc 128:5990–5991
191. Wakahara T, Yamada M, Takahashi S et al (2007) Two-dimensional hopping motion of encapsulated La atoms in silylated La_2@C_{80}. Chem Commun 2680–2682
192. Yamada M, Mizorogi N, Tsuchiya T et al (2009) Synthesis and characterization of the D_{5h} isomer of the endohedral dimetallofullerene Ce_2@C_{80}: two-dimensional circulation of encapsulated metal atoms inside a fullerene cage. Chemistry 15:9486–9493
193. Stevenson S, Rice G, Glass T et al (1999) Small-bandgap endohedral metallofullerenes in high yield and purity. Nature 401:55–57
194. Popov AA, Dunsch L (2007) Structure, stability, and cluster-cage interactions in nitride clusterfullerenes M_3N@C_{2n} (M = Sc, Y; 2n = 68–98): a density functional theory study. J Am Chem Soc 129:11835–11849
195. Rodríguez-Fortea A, Alegret N, Balch AL et al (2010) The maximum pentagon separation rule provides a guideline for the structures of endohedral metallofullerenes. Nat Chem 2:955–961
196. Stevenson S, Phillips JP, Reid JE et al (2004) Pyramidalization of Gd_3N inside a C_{80} cage. The synthesis and structure of Gd_3N@C_{80}. Chem Commun 2814–2815
197. Chaur MN, Melin F, Elliott B et al (2007) Gd_3N@C_{2n} (n = 40, 42, and 44): remarkably low HOMO-LUMO gap and unusual electrochemical reversibility of Gd_3N@C_{88}. J Am Chem Soc 129:14826–14829
198. Chaur MN, Melin F, Ashby J et al (2008) Lanthanum nitride endohedral fullerenes La_3N@C_{2n} (43< or =n< or =55): preferential formation of La_3N@C_{96}. Chemistry 14:8213–8219
199. Cao B, Wakahara T, Maeda Y et al (2004) Lanthanum endohedral metallofulleropyrrolidines: synthesis, isolation, and EPR characterization. Chemistry 10:716–720
200. Cardona CM, Kitaygorodskiy A, Echegoyen L (2005) Trimetallic nitride endohedral metallofullerenes: reactivity dictated by the encapsulated metal cluster. J Am Chem Soc 127:10448–10453
201. Yamada M, Someya C, Wakahara T et al (2008) Metal atoms collinear with the spiro carbon of 6,6-open adducts, M_2@C_{80}(Ad) (M = La and Ce, Ad = adamantylidene). J Am Chem Soc 130:1171–1176
202. Shustova NB, Popov AA, Mackey MA et al (2007) Radical trifluoromethylation of Sc_3N@C_{80}. J Am Chem Soc 129:11676–11677
203. Shu C, Cai T, Xu L et al (2007) Manganese(III)-catalyzed free radical reactions on trimetallic nitride endohedral metallofullerenes. J Am Chem Soc 129:15710–15717
204. Iezzi EB, Duchamp JC, Harich K (2002) A symmetric derivative of the trimetallic nitride endohedral metallofullerene, Sc_3N@C_{80}. J Am Chem Soc 124:524–525
205. Lee HM, Olmstead MM, Iezzi E et al (2002) Crystallographic characterization and structural analysis of the first organic functionalization product of the endohedral fullerene Sc_3N@C_{80}. J Am Chem Soc 124:3494–3495
206. Ge Z, Duchamp JC, Cai T et al (2005) Purification of endohedral trimetallic nitride fullerenes in a single, facile step. J Am Chem Soc 127:16292–16298
207. Cai T, Ge Z, Iezzi EB et al (2005) Synthesis and characterization of the first trimetallic nitride templated pyrrolidino endohedral metallofullerenes. Chem Commun 3594–3596
208. Wakahara T, Iiduka Y, Ikenaga O et al (2006) Characterization of the bis-silylated endofullerene Sc_3N@C_{80}. J Am Chem Soc 128:9919–9925
209. Yamada M, Minowa M, Sato S et al (2011) Regioselective cycloaddition of La_2@I_h-C_{80} with tetracyanoethylene oxide: formation of an endohedral dimetallofullerene adduct featuring enhanced electron-accepting character. J Am Chem Soc 33:3796–3799
210. Liu T-X, Wei T, Zhu S-E et al (2012) Azide addition to an endohedral metallofullerene: formation of azafulleroids of Sc_3N@I_h-C_{80}. J Am Chem Soc 134:11956–11959

211. Yamada M, Nakahodo T, Wakahara T et al (2005) Positional control of encapsulated atoms inside a fullerene cage by exohedral addition. J Am Chem Soc 127:14570–14571
212. Yamada M, Wakahara T, Nakahodo T et al (2006) Synthesis and structural characterization of endohedral pyrrolidinodimetallofullerene: $La_2@C_{80}(CH_2)_2NTrt$. J Am Chem Soc 128:1402–1403
213. Cardona CM, Elliott B, Echegoyen L (2006) Unexpected chemical and electrochemical properties of $M_3N@C_{80}$ (M = Sc, Y, Er). J Am Chem Soc 128:6480–6485
214. Rodríguez-Fortea A, Campanera JM, Cardona CM et al (2006) Dancing on a fullerene surface: isomerization of $Y_3N@$(N-ethylpyrrolidino-C_{80}) from the 6,6 to the 5,6 regioisomers. Angew Chem Int Ed 45:8176–8180
215. Pinzón JR, Plonska-Brzezinska ME, Cardona CM et al (2008) $Sc_3N@C_{80}$-ferrocene electron-donor/acceptor conjugates as promising materials for photovoltaic applications. Angew Chem Int Ed 47:4173–4176
216. Takano Y, Herranz MA, Martín N et al (2010) Donor-acceptor conjugates of lanthanum endohedral metallofullerene and π-extended tetrathiafulvalene. J Am Chem Soc 132:8048–8055
217. Li FF, Pinzón JR, Mercado BQ et al (2011) [2+2]Cycloaddition reaction to $Sc_3N@I_h$-C_{80}. The formation of very stable [5,6]- and [6,6]-adducts. J Am Chem Soc 133:1563–1571
218. Wang GW, Liu TX, Jiao M et al (2011) The cycloaddition reaction of I_h-$Sc_3N@C_{80}$ with 2-amino-4,5-diisopropoxybenzoic acid and isoamyl nitrite to produce an open-cage metallofullerene. Angew Chem Int Ed 50:4658–4662
219. Lukoyanova O, Cardona CM, Rivera J et al (2007) Open rather than closed malonate methano-fullerene derivatives. The formation of methanofulleroid adducts of $Y_3N@C_{80}$. J Am Chem Soc 129:10423–10430
220. Cai T, Xu L, Shu C et al (2008) Selective formation of a symmetric Sc3N@C78 bisadduct: adduct docking controlled by an internal trimetallic nitride cluster. J Am Chem Soc 130:2136–2137
221. Rudolf M, Wolfrum S, Guldi DM et al (2012) Endohedral metallofullerenes–filled fullerene derivatives towards multifunctional reaction center mimics. Chemistry 8:5136–48
222. Feng L, Rudolf M, Wolfrum S et al (2012) A paradigmatic change: linking fullerenes to electron acceptors. J Am Chem Soc 34:12190–12197
223. Li FF, Rodríguez-Fortea A, Poblet JM et al (2011) Reactivity of metallic nitride endohedral metallofullerene anions: electrochemical synthesis of a $Lu_3N@I_h$-C_{80} derivative. J Am Chem Soc 133:2760–2765
224. Li FF, Rodríguez-Fortea A, Peng P et al (2012) Electrosynthesis of a $Sc_3N@I_h$-C_{80} methano derivative from trianionic $Sc_3N@Ih$-C_{80}. J Am Chem Soc 134:480–7487
225. Tsuchiya T, Wielopolski M, Sakuma N et al (2011) Stable radical anions inside fullerene cages: formation of reversible electron transfer systems. J Am Chem Soc 133:13280–13283
226. Armaroli N, Balzani V (2007) The future of energy supply: challenges and opportunities. Angew Chem Int Ed 46:52–66
227. Chapin DM, Fuller CS, Pearson GL (1954) A new silicon *p-n* junction photocell for converting solar radiation into electrical power. J Appl Chem 25:676–678
228. Rispens MT, Hummelen JC (2002) Fullerenes: from synthesis to optoelectronic properties. In: Guldi DM, Martín N (eds) Photovoltaic applications. Kluwer Academic, Dordrech, pp 387–435 (Chap. 12)
229. Hummelen JC, Knight BW, LePeq F et al (1995) Preparation and characterization of fulleroid and methanofullerene derivatives. J Org Chem 60:532–538
230. Yu G, Gao J, Hummelen JC et al (1995) Polymer photovoltaic cells: enhanced efficiencies via a network of internal donor-acceptor heterojunctions. Science 270:1789–1791
231. Zhang Y, Yip HL, Acton O et al (2009) A simple and effective way of achieving highly efficient and thermally stable bulk-heterojunction polymer solar cells using amorphous fullerene derivatives as electron acceptor. Chem Mater 21:2598–2600

232. Lenes L, Wetzelaer GJAH, Kooistra FB et al (2008) Fullerene bisadducts for enhanced open-circuit voltages and efficiencies in polymer solar cells. Adv Mater 20:2116–2119
233. Wienk MM, Kroon JM, Verhees WJH et al (2003) Efficient methano[70]fullerene/MDMO-PPV bulk heterojunction photovoltaic cells. Angew Chem Int Ed 42:3371–3375
234. Park SH, Roy A, Beaupré S et al (2009) Bulk heterojunction solar cells with internal quantum efficiency approaching 100%. Nat Photonics 3:297–302
235. Kooistra FB, Mihailetchi VD, Popescu LM et al (2006) New C_{84} derivative and its application in a bulk heterojunction solar cell. Chem Mater 18:3068–3073
236. Li CZ, Yip HL, Jen AKY (2012) Functional fullerenes for organic photovoltaics. J Mater Chem 22:4161–4177
237. Riedel I, von Hauff E, Parisi J et al (2005) Diphenylmethanofullerenes: new and efficient acceptors in bulk-heterojunction solar cells. Adv Funct Mater 15:1979–1987
238. Riedel I, Martín N, Giacalone F et al (2004) Polymer solar cells with novel fullerene-based acceptor. Thin Solid Films 451:43–47
239. Backer S, Sivula K, Kavulak DF et al (2007) High efficiency organic photovoltaics incorporating a new family of soluble fullerene derivatives. Chem Mater 19:2927–2929
240. He Y, Chen HY, Hou J et al (2010) Indene–C_{60} bisadduct: a new acceptor for high-performance polymer solar cells. J Am Chem Soc 132:1377–1382
241. Weiss EA, Wasielewski MR, Ratner MA (2005) Molecules as wires: molecule-assisted movement of charge and energy. Top Curr Chem 257:103–133
242. Guldi DM, Illescas BM, Atienza CM et al (2009) Fullerene for organic electronics. Chem Soc Rev 38:1587–1597
243. Ito O, Yamanaka K (2009) Roles of molecular wires between fullerenes and electron donors in photoinduced electron transfer. Bull Chem Soc Jpn 82:316–332
244. Vail SA, Schuster DI, Guldi DM et al (2006) Energy and electron transfer in beta-alkynyl-linked porphyrin-[60]fullerene dyads. J Phys Chem B 110:14155–14166
245. Vail SA, Krawczuk PJ, Guldi DM et al (2005) Energy and electron transfer in polyacetylene-linked zinc–porphyrin–[60]fullerene molecular wires. Chemistry 11:3375–3388
246. Tashiro K, Sato A, Yuzawa T et al (2006) Long-range photoinduced electron transfer mediated by oligo-p-phenylenebutadiynylene conjugated bridges. Chem Lett 35:518–519
247. Lembo A, Tagliatesta P, Guldi DM et al (2009) Porphyrin-β-oligo-ethynylenephenylene-[60] fullerene triads: synthesis and electrochemical and photophysical characterization of the new porphyrin-oligo-PPE-[60]fullerene systems. J Phys Chem A 113:1779–1793
248. Giacalone F, Segura JL, Martín N et al (2004) Exceptionally small attenuation factors in molecular wires. J Am Chem Soc 126:5340–5341
249. Giacalone F, Segura JL, Martín N et al (2005) Probing molecular wires: synthesis, structural, and electronic study of donor-acceptor assemblies exhibiting long-range electron transfer. Chemistry 11:4819–4834
250. de la Torre G, Giacalone F, Segura JL et al (2005) Electronic communication through π-conjugated wires in covalently linked porphyrin/C_{60} ensembles. Chemistry 11:12671280
251. Molina-Ontoria A, Wielopolski M, Gebhardt J (2011) [2,2′]Paracyclophane-based π-conjugaed molecular wires reveal molecular-junction behavior. J Am Chem Soc 133:2370–2373
252. Atienza-Castellanos C, Wielopolski M, Guldi DM et al (2007) Determination of the attenuation factor in fluorene-based molecular wires. Chem Commun 5164–5166
253. Wielopolski M, Santos J, Illescas BM et al (2011) Vinyl spacers – tuning electron transfer through fluorene-based molecular wires. Energy Environ Sci 4:765–771
254. Ikemoto J, Takimiya K, Aso Y et al (2002) Porphyrin–oligothiophene–fullerene triads as an efficient intramolecular electron-transfer system. Org Lett 4:309–311
255. Nakamura T, Fujitsuka M, Araki Y et al (2004) Photoinduced electron transfer in porphyrin-oligothiophene-fullerene linked triads by excitation of a porphyrin moiety. J Phys Chem B 108:10700–10710
256. Wessendorf F, Grimm B, Guldi DM et al (2010) Pairing fullerenes and porphyrins: supramolecular wires that exhibit charge transfer activity. J Am Chem Soc 132:10786–10795

257. Schmalz TG, Seitz WA, Klein DJ et al (1986) C_{60} carbon cages. Chem Phys Lett 130:203–207
258. Schein S, Friedrich TA (2008) A geometric constraint, the head-to-tail exclusion rule, may be the basis for the isolated-pentagon rule in fullerenes with more than 60 vertices. Proc Natl Acad Sci U S A 105:19142–19147
259. Tan T-Z, Li J, Zhu F et al (2010) Chlorofullerenes featuring triple sequentially fused pentagons. Nat Chem 2:269–273
260. Martín N (2011) Fullerene $C_{72}Cl_4$: the exception that proves the rule? Angew Chem Int Ed 50:5431–5433
261. Tan Y-Z, Xie S-Y, Huang R-B et al (2009) The stabilization of fused-pentagon fullerene molecules. Nat Chem 1:450–460
262. Wang CR, Kai T, Tomiyama T et al (2000) Materials science – C_{66} fullerene encaging a scandium dimer. Nature 408:426–427
263. Stevenson S, Fowler PW, Heine T et al (2000) Materials science: a stable non-classical metallofullerene family. Nature 408:427–428
264. Beavers CM, Zuo TM, Duchamp JC et al (2006) $Tb_3N@C_{84}$: an improbable, egg-shaped endohedral fullerene that violates the isolated pentagon rule. J Am Chem Soc 128:11352–11353
265. Yang SF, Popov AA, Dunsch L (2007) Violating the isolated pentagon rule (IPR): the endohedral non-IPR C_{70} cage of $Sc_3N@C_{70}$. Angew Chem Int Ed 46:1256–1259
266. Ma YH, Wang TS, Wu JY et al (2011) Size effect of endohedral cluster on fullerene cage: preparation and structural studies of $Y_3N@C_{78}$-C_2. Nanoscale 3:4955–4957
267. Shi ZQ, Wu X, Wang CR et al (2006) Isolation and characterization of $Sc_2C_2@C_{68}$: a metal-carbide endofullerene with a non-IPR carbon cage. Angew Chem Int Ed 45:2107–2111
268. Wu JY, Wang TS, Ma YH et al (2011) Synthesis, isolation, characterization, and theoretical studies of $Sc_3NC@C_{78}$-C_2. J Phys Chem C 115:23755–23759
269. Campanera JM, Bo C, Poblet JM (2005) General rule for the stabilization of fullerene cages encapsulating trimetallic nitride templates. Angew Chem Int Ed 44:7230–7233
270. Summerscales OT, Cloke FGN (2006) The organometallic chemistry of pentalene. Coord Chem Rev 250:1122–1140
271. Xie SY, Gao F, Lu X et al (2004) Capturing the labile fullerene[50] as $C_{50}Cl_{10}$. Science 304:699–699
272. Wang CR, Shi ZQ, Wan LJ et al (2006) C64H4: production, isolation, and structural characterizations of a stable unconventional fulleride. J Am Chem Soc 128:6605–6610
273. Li B, Shu CY, Lu X et al (2010) Addition of carbene to the equator of C(70) to produce the most stable C(71)H(2) isomer: 2 aH-2(12)a-homo(C(70)-D(5 h(6)))[5,6]fullerene. Angew Chem Int Ed 49:962–966
274. Tan YZ, Li J, Zhou T, Feng YQ et al (2010) Pentagon-fused hollow fullerene in C_{78} family retrieved by chlorination. J Am Chem Soc 132:12648–12652
275. Kato H, Taninaka A, Sugai T et al (2003) Structure of a missing-caged metallofullerene: $La_2@C_{72}$. J Am Chem Soc 125:7782–7783
276. Yamada M, Wakahara T, Tsuchiya T et al (2008) Spectroscopic and theoretical study of endohedral dimetallofullerene having a non-IPR fullerene cage: $Ce_2@C_{72}$. J Phys Chem A 112:7627–7631
277. Wakahara T, Nikawa H, Kikuchi T et al (2006) $La@C_{72}$ having a non-IPR carbon cage. J Am Chem Soc 128:14228–14229
278. Chen N, Beavers CM, Mulet-Gas M et al (2012) $Sc_2S@C(s)(10528)$-C_{72}: a dimetallic sulfide endohedral fullerene with a non isolated pentagon rule cage. J Am Chem Soc 134:7851–7860
279. Tan Y-Z, Zhou T, Bao J, Shan G-J, Xie S-Y, Huang R-B, Zheng L-S (2010) $C_{72}Cl_4$: a pristine fullerene with favorable pentagon-adjacent structure. J Am Chem Soc 132:17102–17104
280. Ziegler K, Mueller A, Amsharov KY, Jansen M (2010) Disclosure of the elusive C_{2v}-C_{72} carbon cage. J Am Chem Soc 132:17099–17101